In situ measurements of hydrogen sulfide, oxygen, and temperature in diffuse fluids of an ultramafic-hosted hydrothermal vent field (Logatchev, 14 degrees 45 ' N, Mid-Atlantic Ridg...

Article *in* Geochemistry Geophysics Geosystems · September 2011

DOI: 10.1029/2011GC003632

CITATIONS
22

READS
482

5 authors, including:

Christian Borowski
Max Planck Institute for Marine Microbiology
69 PUBLICATIONS **1,677** CITATIONS
SEE PROFILE

Frank Wenzhoefer
Alfred Wegener Institute Helmholtz Centre for Polar and Marine Research
189 PUBLICATIONS **4,786** CITATIONS
SEE PROFILE

Nicole Dubilier
Max Planck Institute for Marine Microbiology
152 PUBLICATIONS **5,641** CITATIONS
SEE PROFILE

Geochemistry Geophysics Geosystems G3

Article
Volume 12, Number 9
16 September 2011
Q0AE04, doi:10.1029/2011GC003632
ISSN: 1525-2027

Published by AGU and the Geochemical Society

In situ measurements of hydrogen sulfide, oxygen, and temperature in diffuse fluids of an ultramafic-hosted hydrothermal vent field (Logatchev, 14°45′N, Mid-Atlantic Ridge): Implications for chemosymbiotic bathymodiolin mussels

Frank U. Zielinski
Symbiosis Group, Max Planck Institute for Marine Microbiology, Celsiusstr. 1, D-28359 Bremen, Germany

Department of Environmental Microbiology, Helmholtz-Centre for Environmental Research–UFZ, Permoserstraße 15, D-04318 Leipzig, Germany (frank.zielinski@ufz.de)

Hans-Hermann Gennerich
Marine Technology–Sensors, Department of Geosciences, University of Bremen, Klagenfurter Str., D-28334 Bremen, Germany (hherm@uni-bremen.de)

Christian Borowski
Symbiosis Group, Max Planck Institute for Marine Microbiology, Celsiusstr. 1, D-28359 Bremen, Germany (cborowsk@mpi-bremen.de)

Frank Wenzhöfer
Habitat Group, Max Planck Institute for Marine Microbiology, Celsiusstr. 1, D-28359 Bremen, Germany (fwenzhoe@mpi-bremen.de)

Research Group on Deep-Sea Ecology and Technology, Alfred Wegener Institute for Polar and Marine Research, PO Box 120161, D-27515 Bremerhaven, Germany

Nicole Dubilier
Symbiosis Group, Max Planck Institute for Marine Microbiology, Celsiusstr. 1, D-28359 Bremen, Germany (ndubilie@mpi-bremen.de)

[1] The Logatchev hydrothermal vent field (14°45′N, Mid-Atlantic Ridge) is located in a ridge segment characterized by mantle-derived ultramafic outcrops. Compared to basalt-hosted vents, Logatchev high-temperature fluids are relatively low in sulfide indicating that the diffuse, low-temperature fluids of this vent field may not contain sufficient sulfide concentrations to support a chemosymbiotic invertebrate community. However, the high abundances of bathymodiolin mussels with bacterial symbionts related to free-living sulfur-oxidizing bacteria suggested that bioavailable sulfide is present at Logatchev. To clarify, if diffuse fluids above mussel beds of *Bathymodiolus puteoserpentis* provide the reductants and oxidants needed by their symbionts for aerobic sulfide oxidation, in situ microsensor measurements of dissolved hydrogen sulfide and oxygen were combined with simultaneous temperature measurements. High temporal fluctuations of all three parameters were measured above the mussel beds. H_2S and O_2 coexisted with mean concentrations between 9 and 31 μM (H_2S) and 216 and 228 μM (O_2). Temperature maxima (≤7.4°C) were generally concurrent with H_2S maxima (≤156 μM) and O_2 minima (≥142 μM). Long-term measurements for 250 days using temperature as a proxy for oxygen and sulfide concentrations indicated that the mussels

were neither oxygen limited nor sulfide limited. Our in situ measurements at Logatchev indicate that sulfide may also be bioavailable in diffuse fluids from other ultramafic-hosted vents along slow and ultraslow spreading ridges.

Components: 12,100 words, 9 figures, 4 tables.

Keywords: Bathymodiolus puteoserpentis; Logatchev hydrothermal vent field; hydrothermal diffuse flow; microsensors; ultramafic-hosted hydrothermal vents.

Index Terms: 4811 Oceanography: Biological and Chemical: Chemosynthesis; 4832 Oceanography: Biological and Chemical: Hydrothermal systems (0450, 1034, 3017, 3616, 8135, 8424); 4835 Oceanography: Biological and Chemical: Marine inorganic chemistry (1050); 4872 Oceanography: Biological and Chemical: Symbiosis; 4894 Oceanography: Biological and Chemical: Instruments, sensors, and techniques.

Received 23 March 2011; **Revised** 24 June 2011; **Accepted** 30 June 2011; **Published** 16 September 2011.

Zielinski, F. U., H.-H. Gennerich, C. Borowski, F. Wenzhöfer, and N. Dubilier (2011), In situ measurements of hydrogen sulfide, oxygen, and temperature in diffuse fluids of an ultramafic-hosted hydrothermal vent field (Logatchev, 14°45′N, Mid-Atlantic Ridge): Implications for chemosymbiotic bathymodiolin mussels, *Geochem. Geophys. Geosyst.*, *12*, Q0AE04, doi:10.1029/2011GC003632.

Theme: From the Mantle to the Ocean: Life, Energy, and Material Cycles at Slow Spreading Ridges
Guest Editors: C. Devey, N. Dublilier, J. Lin, N. Le Bris, and D. Connelly

1. Introduction

[2] Hydrothermal vents along oceanic spreading ridges occur in different types of geological settings. According to the prevailing rock types that characterize the ocean floor, vents have been classified as basalt hosted, ultramafic hosted, felsic hosted, or sediment hosted [*Tivey*, 2007]. Vents on mid-ocean ridges with ultrafast to intermediate spreading rates occur exclusively in basalt-hosted settings in which the upper oceanic crust is composed entirely of basaltic rocks [*Wetzel and Shock*, 2000]. In contrast, vents on slow and ultraslow spreading mid-ocean ridges are either basalt or ultramafic hosted. In ultramafic-hosted settings, the upper oceanic crust is composed mainly of mantle-derived peridotite [*Cannat et al.*, 1997; *Snow and Edmonds*, 2007; *Tivey*, 2007; *Wetzel and Shock*, 2000]. Ultramafic systems are now known to occur more often than previously recognized along slow and ultraslow spreading ridges [*Beaulieu*, 2010; *Snow and Edmonds*, 2007]. Back-arc basin spreading centers are common in the West Pacific where the host rock composition can be felsic (consisting of andesite, rhyolite, and dacite) as well as basaltic [*Martinez et al.*, 2007; *Tivey*, 2007]. Finally, hydrothermal settings can also be sediment hosted if they are associated with ridges close to continental margins, such as numerous vent fields along the west coast of North America [*Tivey*, 2007; *Tunnicliffe et al.*, 1998].

[3] Basaltic, ultramafic, felsic and sedimentary rocks react differently with subsurface seawater, which leads to differences in the fluid composition [*German and Von Damm*, 2006; *Tivey*, 2007]. In this paper we focus on basalt- and ultramafic-hosted systems along mid-ocean ridges. High-temperature hydrothermal fluids discharged from basalt-hosted systems have total sulfide concentrations (S_{tot} = $H_2S + HS^- + FeS + S_x^{2-}$) as high as 20 mM that can temporarily rise to as high as 30–110 mM during a magmatic event [*German and Von Damm*, 2006; *Lilley et al.*, 2003; *Tivey*, 2007]. In contrast, high-temperature fluids from ultramafic-hosted systems such as Rainbow (36°14′N) and Logatchev (14°45′N) on the Mid-Atlantic Ridge (MAR) have high concentrations of dissolved hydrogen (12–19 mM) and methane (2.1–3.5 mM) but relatively lower total sulfide concentrations (0.8–2.5 mM) [*Charlou et al.*, 2002; *Douville et al.*, 2002; *Schmidt et al.*, 2007]. Correspondingly, discrete sampling of Rainbow and Logatchev low-temperature diffuse fluids followed by shipboard analysis indicated only low total sulfide concentrations (S_{tot} at Rainbow: ≤ 22 μM) with the exception of a single measurement of 70 μM free or bioavailable sulfide (S_{free} = $H_2S + HS^-$) in Logatchev diffuse fluids [*Geret et al.*, 2002; *Schmidt et al.*, 2007]. In situ measurements con-

firmed the low sulfide content in Rainbow diffuse fluids (S_{tot} < 5 μM) [*Le Bris and Duperron*, 2010; *Schmidt et al.*, 2008], which suggests that only very little bioavailable sulfide is present in diffuse fluids from ultramafic-hosted vents (see section 2 for definitions of total and bioavailable sulfide). Beyond the study by *Schmidt et al.* [2008] at Rainbow, which focused only on habitats where the vent shrimps *Rimicaris exoculata* occur (habitat temperatures between 5°C and 18°C), no in situ sulfide concentrations of fluids from ultramafic-hosted vent sites have been published.

[4] In contrast, at basalt-hosted vents sulfide concentrations have frequently been measured in situ, for example at the intermediate spreading Galapagos Rift [*Fisher et al.*, 1988; *Johnson et al.*, 1986b, 1994, 1988b] and the fast spreading East Pacific Rise [*Di Meo-Savoie et al.*, 2004; *Le Bris et al.*, 2003, 2005, 2006b; *Luther et al.*, 2001a, 2001b, 2008; *Lutz et al.*, 2008; *Moore et al.*, 2009; *Nees et al.*, 2009, 2008; *Rozan et al.*, 2000]. Maxima of up to 330 μM (S_{tot}) and a mean of 27 μM were measured over *Bathymodiolus thermophilus* mussel beds at the Galapagos Rift [*Fisher et al.*, 1988; *Johnson et al.*, 1994, 1988b]. Tubeworms generally occur at diffuse fluids with higher temperatures than those inhabited by bathymodiolin mussels, and correspondingly, sulfide maxima as high as 500 μM (S_{free}) and means of 12–112 μM were recorded in *Riftia pachyptila* and *Tevnia jerichonana* tubeworm habitats on the East Pacific Rise [*Nees et al.*, 2009]. At basalt-hosted vents on the slow spreading Mid-Atlantic Ridge, only a few in situ measurements of sulfide are available, and concentrations of up to 67 μM (S_{tot}) were measured over *B. azoricus* mussel beds (mean 9 μM) [*Desbruyères et al.*, 2001; *Le Bris and Duperron*, 2010; *Le Bris et al.*, 2000; *Vuillemin et al.*, 2009]. Recently, in situ sulfide data were also published for the basalt- and andesite-hosted Eastern Lau Spreading Center in the West Pacific where up to 130 μM (S_{free}) was measured over *B. brevior* mussel beds with means of 8–24 μM [*Mullaugh et al.*, 2008; *Podowski et al.*, 2009, 2010; *Waite et al.*, 2008].

[5] At Logatchev, dense beds of the deep-sea mussel *Bathymodiolus puteoserpentis* [*Maas et al.*, 1999; *von Cosel et al.*, 1999] cover areas where diffuse fluids emerge from the subsurface. These mussels harbor two types of bacterial symbionts in their gills, methane oxidizers and sulfur oxidizers (also known as methanotrophic and thiotrophic symbionts) [*Duperron et al.*, 2006]. The high methane concentrations in the end-member fluids of this ultramafic-hosted vent [*Charlou et al.*, 2002; *Schmidt et al.*, 2007] indicate sufficient quantities of methane for endosymbiotic methanotrophy. However, the lack of data on in situ concentrations of sulfide at ultramafic-hosted vents raises the question if enough free sulfide (H_2S + HS^-) is available to support the thiotrophic symbionts of *B. puteoserpentis*. In this study we combined in situ measurements of dissolved hydrogen sulfide (H_2S), oxygen, and temperature over *B. puteoserpentis* mussel beds using amperometric H_2S microsensors [*Jeroschewski et al.*, 1996; *Kühl et al.*, 1998], Clark-type O_2 microsensors [*Revsbech*, 1989] and temperature sensors. We compare the results with data from the ultramafic-hosted Rainbow field as well as basalt-hosted hydrothermal vent systems and discuss their implications for chemosymbiotic bathymodiolin mussels.

2. Material and Methods

2.1. Study Site

[6] The ultramafic-hosted Logatchev hydrothermal vent field is located at 14°45′N and 44°58′W on the Mid-Atlantic Ridge at a water depth of 2910–3060 m (Figure 1). The geological setting of this field has been described in detail by *Bogdanov et al.* [1997], *Gebruk et al.* [2000], and *Petersen et al.* [2009]. Here we provide a short summary of the six sites we investigated in this study, Sites 1–5 at Irina II and Site 6 at Irina I.

[7] Irina II is a mound with a basal diameter of about 50 × 25 m and steep slopes rising about 15 m above the surrounding seafloor. Five vertical up to 3 m high smoker chimneys at the top of the mound rather slowly emanate black smoke [*Petersen et al.*, 2009] (Figure 1). Diffuse flow escapes through the chimney walls of beehive and pillar-like sulfide structures. The Irina II mound is densely covered with mussels [*Petersen et al.*, 2009]. A single mussel bed of at least 20 m diameter extends from the base to the top of the central smoker complex [*Gebruk et al.*, 2000]. In addition, the mound is surrounded by smaller mussel beds (up to 3 × 4 m) and mussel patches of 20–30 cm in diameter. These mussel beds are inhabited by polychaetes, gastropods (snails and limpets), alvinocarid shrimps, crabs, and large numbers of brittle stars [*Gebruk et al.*, 2010, 2000; *Van Dover and Doerries*, 2005]. A single highly active black smoker rises at the southeastern end of the mound [*Petersen et al.*, 2009].

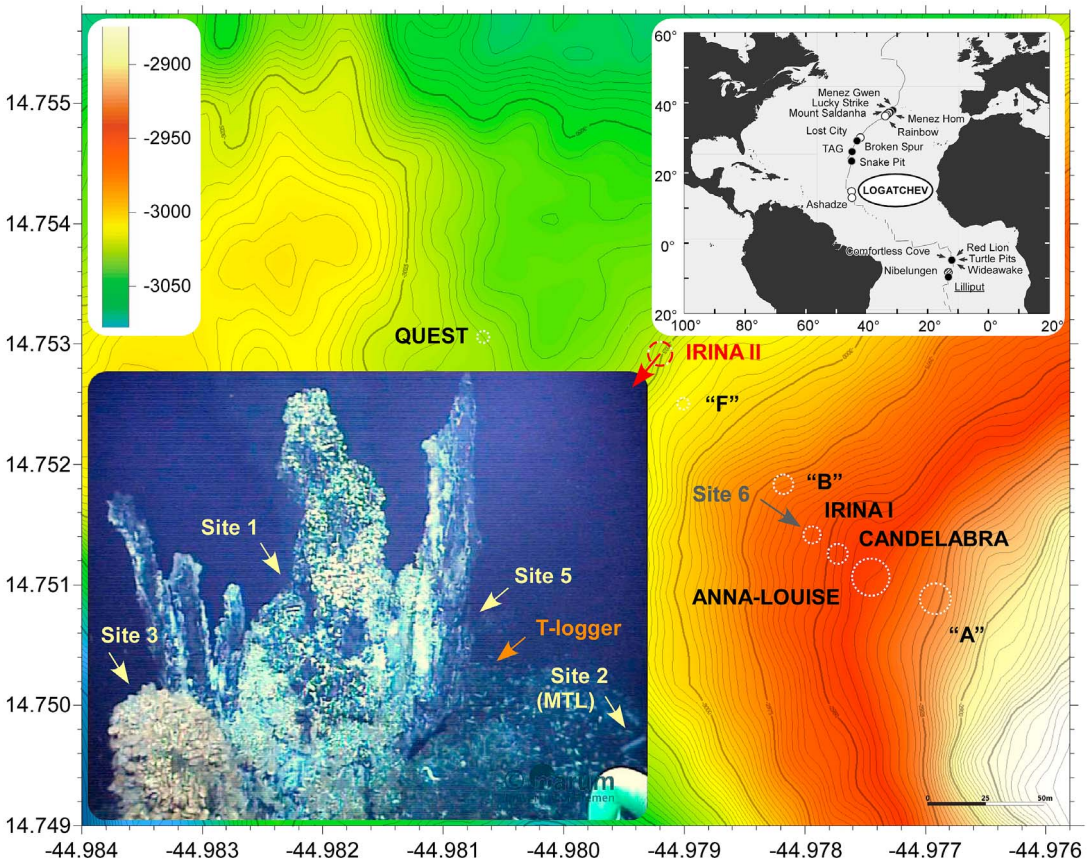

Figure 1. Map of the Logatchev hydrothermal vent field. The Irina II site where most measurements were performed is highlighted in red. The gray arrow points to Site 6 at Irina I. Map modified from *Borowski et al.* [2008]. (bottom inset) View of the Irina II hydrothermal main structure from NW (copyright, MARUM University of Bremen). The yellow arrows indicate where in situ measurements were performed. Site 1, chimney on the top of the main structure; Site 2, lower end of the main mussel bed at the western slope of the main structure (MTL, miniaturized temperature logger); Site 3, pillar-like structure densely overgrown with mussels; Site 4 (not shown), a small mussel patch at the base of the main structure; Site 5, chimney structure populated with swarms of shrimp but without mussels. Orange arrow indicates the deployment site of the multichannel long-term temperature logger within the mussel bed. (top inset) Map showing the Logatchev hydrothermal vent field in relation to known hydrothermal vent fields along the Mid-Atlantic Ridge. White circles indicate ultramafic-hosted vent fields, and black circles indicate basalt-hosted vent fields.

[8] Irina I is characterized by smoking craters, emanating high-temperature fluids, structures that are only known from the Logatchev vent field. Small chimneys occur on the crater rims and black smoke is intensively vented either from the chimneys on the crater rim or from holes in the ground within the craters [*Petersen et al.*, 2009]. Meter-wide bacterial mats grow at the northwestern part of Irina I, but animals are scarce and mainly consist of actinians and hydrozoans in the vicinity of the outer crater rim, while mussels are completely absent [*Kuhn et al.*, 2004].

[9] Four mussel habitats at Irina II were investigated in terms of the chemical energy supply from diffuse venting: (1) a colonized chimney on the top of the main structure (Site 1), (2) the lower end of the main mussel bed covering the western slope of the mound (Site 2), (3) an overgrown sulfide pillar on the main structure (Site 3), and (4) a small mussel patch at the base of the mound (Site 4). Additionally, two sites without mussels were investigated: a chimney wall on the main structure covered with alvinocarid shrimp (Site 5) and the rim of a smoking crater at the Irina I site (Site 6), 230 m southeast of Irina II [*Borowski et al.*, 2008].

2.2. Methods for Measuring Sulfide in Situ

[10] Two basic principles have been used over the last two decades to determine in situ sulfide concentrations in hydrothermal diffuse flow: colorimetry and

electrochemistry [see also *Le Bris and Duperron*, 2010]. Colorimetric detection was initially based on conventional flow analysis [*Johnson et al.*, 1986a; *Massoth and Milburn*, 1997; *Sakamoto-Arnold et al.*, 1986] and was later replaced by flow injection analysis [*Le Bris et al.*, 2000; *Sarradin et al.*, 1999a; *Vuillemin et al.*, 2009]. Colorimetry measures the total sulfide concentration (S_{tot}), which is the sum of several different sulfide species such as dissolved H_2S, HS^-, and labile metal sulfides ($S_{tot} = H_2S + HS^- + FeS + S_x^{2-}$). At hydrothermal vents the concentration of labile metal sulfides can be quite high [*German and Von Damm*, 2006]. Although these metal sulfides can be exploited by some free-living sulfur-oxidizing microorganisms they cannot be used by symbiotic sulfur oxidizers of vent invertebrates, which dominate the biomass at deep-sea hydrothermal vents [*Van Dover*, 2000]. Therefore, total sulfide values do not reflect the sulfide species that are biologically relevant or bioavailable for symbiotic sulfur oxidizers, i.e., H_2S and HS^- (free sulfide or S_{free}).

[11] In contrast to colorimetric methods, electrochemical sensors can distinguish between different sulfide species. They relate an electrochemically induced change of the electric current between a working electrode and a counter electrode, both polarized at different potentials against a reference electrode, to the in situ concentration of the investigated sulfur species. Voltammetric sensors can detect and distinguish between free sulfide ($S_{free} = H_2S + HS^-$), soluble iron-sulfide clusters (FeS_{aq}), elemental sulfur (S^0), polysulfides (S_x^{2-}), thiosulfate ($S_2O_3^{2-}$), and tetrathionate ($S_4O_6^{2-}$) [*Di Meo-Savoie et al.*, 2004; *Luther et al.*, 2001a, 2001b, 2008; *Mullaugh et al.*, 2008; *Rozan et al.*, 2000; *Waite et al.*, 2008]. In contrast, amperometric sensors detect sulfide exclusively in its undissociated form as dissolved gaseous hydrogen sulfide (H_2S), but the concentration of HS^- can be calculated if the pH is measured simultaneously. The principle of H_2S detection is based on the ferricyanide/ferrocyanide ($[Fe(CN)_6]^{3-}/[Fe(CN)_6]^{4-}$) redox couple. H_2S diffuses via a silicone membrane (permeable only for uncharged molecules, high gas permeability) and is oxidized by ferricyanide resulting in the formation of elemental sulfur and ferrocyanide. The latter is electrochemically reoxidized thereby creating a current that is directly proportional to the dissolved H_2S concentration [*Jeroschewski et al.*, 1996; *Kühl et al.*, 1998].

[12] The purpose of our study was to examine if free sulfide ($H_2S + HS^-$) is available in sufficient concentrations to support the thiotrophic symbionts of *B. puteoserpentis* mussels. As metal sulfide concentrations are relatively high at ultramafic-hosted hydrothermal systems [*Douville et al.*, 2002; *German and Von Damm*, 2006], the colorimetric detection of sulfide would likely severely bias sulfide bioavailability results [*Le Bris et al.*, 2003]. In contrast, both electrochemical methods are suitable for identifying the bioavailable portion of sulfides. Since in situ voltammetry was not available, we chose the amperometric approach along with pH detection. Amperometric H_2S microsensors have not been used previously at deep-sea hydrothermal vents and were deployed in hydrothermal diffuse flow for the first time in this study.

2.3. Combined in Situ Measurements of Dissolved Hydrogen Sulfide, Dissolved Oxygen, and Temperature

[13] In situ measurements of dissolved hydrogen sulfide, dissolved oxygen, and temperature were performed in 2004 during the Hydromar I cruise with the R/V *Meteor* (M60/3 [*Kuhn et al.*, 2004]). All measurements were recorded for 2 to 5 min at the six different study sites (Figure 1 and Table 1). The sulfide, oxygen, and temperature sensors were connected to a custom-built in situ instrument (ISI). The ISI is identical to the autonomous microprofiler used previously in sedimented environments [*de Beer et al.*, 2006; *Wenzhöfer and Glud*, 2002; *Wenzhöfer et al.*, 2000] but here measurements were conducted semiautonomously on four dives using the ROV Quest (MARUM, Bremen, Germany; Table 1). The ISI was fastened horizontally on an extendable drawer underneath the ROV, with the sensor tips protruding from the drawer. To prevent damage, the sensors were surrounded by a protective cage made of titanium bars bolted on robust Teflon discs. The cage allowed seawater and diffuse fluids to pass freely to the sensors (Figures 2a and 2b). Power supply and data exchange between the instrument and the ROV was enabled via a SeaNet Cable/Connector System (Schilling Robotics, Davis, California). Data were recorded every second during the entire dive. During measurements the ROV remained in a fixed position and the ROV drawer with the instrument was horizontally extended so that the sensor tips were positioned as close as possible to the mussel beds (Figure 2b). Due to the technical setup and the horizontal ISI deployment mode, H_2S and O_2 microsensors were typically positioned between 5 and 13 cm above the beds while the temperature sensor was located between 7 and 11 cm above the mussels. All data were stored in the ISI internal memory as well as in the central

Table 1. Location of in Situ Measurements

Location	Designation	Dive	Date	Time (UTC)[a]	Depth (m)	Figure
Chimney base colonized with mussels	Site 1a	9 (38ROV)	26 Jan 2004	17:00–19:00	3035	Figure 5a
Chimney top colonized with mussels	Site 1b	9 (38ROV)	26 Jan 2004	19:00–20:15	3034	Figure 5a
Mussel bed	Site 2	9 (38ROV)	26 Jan 2004	15:30–16:20	3035	Figure 5b
Sulfide pillar overgrown with mussels	Site 3	9 (38ROV)	26 Jan 2004	16:20–17:05	3035	Figure 5c
Mussel patch	Site 4a	14 (66ROV)	03 Feb 2004	18:46–19:01	3052	Figure 5d
Mussel patch	Site 4b	14 (66ROV)	03 Feb 2004	20:01–20:08	3053	Figure 5d
Chimney wall populated with shrimp	Site 5	8 (29ROV)	24 Jan 2004	16:49–17:02	3033	Figure 5e
Rim of smoking crater	Site 6	14 (66ROV)	03 Feb 2004	16:50–17:55	2961	Figure 3

[a]UTC, universal time code.

ROV database and downloaded for analysis at the end of the dive.

2.4. Sensors, Calibration, and Data Analysis

[14] All sensors were calibrated before each dive. Dissolved H_2S was measured with amperometric H_2S microelectrodes (response time (t_{90}) < 0.5 s; stirring sensitivity < 2%; detection limit ~ 2 μM) as described by *Jeroschewski et al.* [1996] and *Kühl et al.* [1998]. The sensors were calibrated according to previously published methods in an anoxic phosphate buffer solution (pH 7.5, 200 mM) by stepwise addition of discrete amounts of a 1.3 M Na_2S stock solution [*de Beer et al.*, 2006; *Wenzhöfer et al.*, 2000]. To determine concentrations of total dissolved sulfide [S_{tot}] subsamples were taken, fixed in acidic 5% (w/v) zinc acetate solution, and stored at 4°C in the dark until further analysis. The resulting ZnS precipitate concentration was measured spectrophotometrically at 670 nm using the methy-

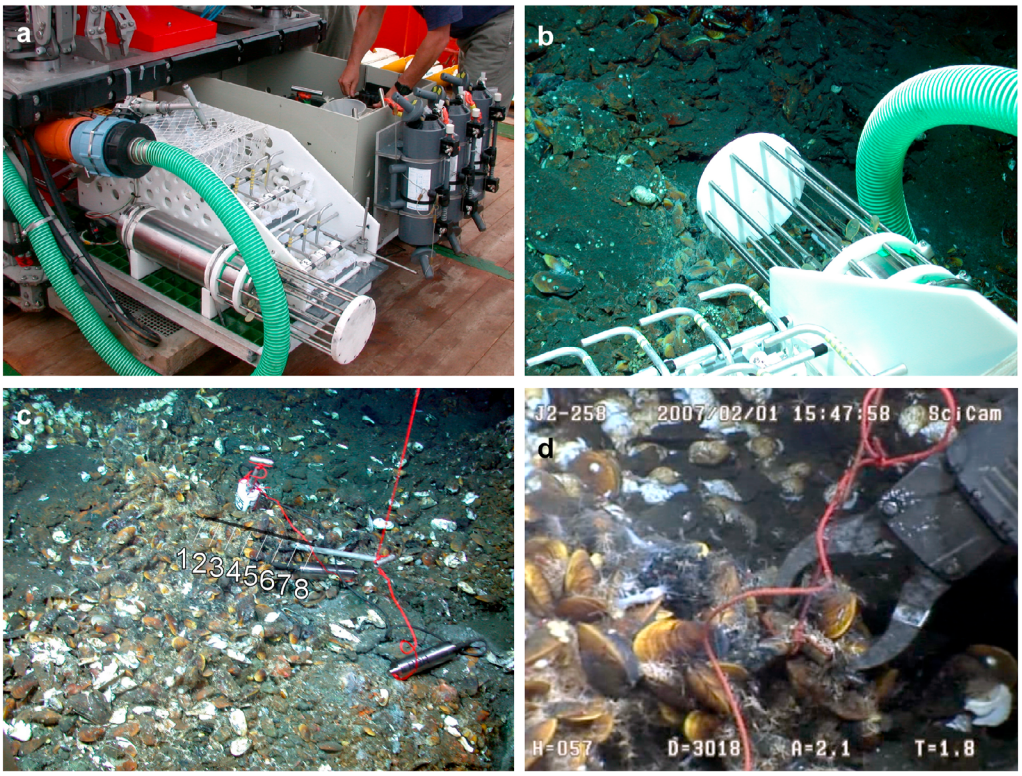

Figure 2. In situ instrument (ISI) and 8-channel temperature lances. (a) ISI setup on the extendable drawer of the ROV Quest (left). (b) ISI taking measurements on above a small mussel patch at Site 4. Copyright, MARUM University of Bremen. (c) T-logger site with two 8-channel temperature lances pushed horizontally (at an angle of about 20°) and vertically into the mussel bed. The black line indicates the position of the horizontal temperature lance within the mussel bed, while 1–8 marks the position of the temperature sensors inside the lance. Copyright, MARUM University of Bremen. (d) Recovery of the horizontal temperature lance. Copyright, Woods Hole Oceanographic Institute.

lene blue method according to *Cline* [1969]. The H_2S concentrations in the subsamples were calculated as described by *Jeroschewski et al.* [1996] using equation (1) where pK_1^* is the negative decadal logarithm of the first dissociation constant of the sulfide equilibrium K_1 corrected for salinity according to *Millero et al.* [1988]. The salinity of the phosphate buffer was 27‰ as determined with a refractometer.

$$[H_2S] = \frac{[S_{tot}^{2-}]}{1 + 10^{(pH - pK_1^*)}} \quad (1)$$

To account for the varying in situ temperatures at the hydrothermal vent, the calibration was performed at least at two temperatures.

[15] Dissolved O_2 was measured with Clark type microelectrodes (response time (t_{90}) < 1 s; stirring sensitivity < 1%) [*Revsbech*, 1989]. The sensors were calibrated in seawater bubbled with nitrogen gas for anoxic and air for oxic calibrations. The O_2 concentrations for saturation were calculated according to *Weiss* [1970]. To account for the sensor's temperature sensitivity, the sensors were calibrated at two to three different temperatures.

[16] Temperature was measured with a Pt100 stainless steel sensor (UST Umweltsensortechnik Geschwenda, Germany) at a resolution of 0.01°C. The sensor was calibrated at eight temperatures between 1 and 78°C by comparison with a commercial digital thermometer.

[17] To relate the microsensor signals to the dissolved gas concentration, a calibration curve was calculated for each calibration temperature using linear regression based on the least squares method. To account for in situ temperatures, regression equations for any virtual temperature were calculated from both the slopes and intercepts computed for the calibration temperatures. From these equations the calibration formulas for temperatures from 2.5 to 27°C were calculated with a resolution of 0.01°C. These formulas were fine-tuned by relating them to in situ background sensor signals. The H_2S calibration formulas were corrected for the sensor signal recorded outside the hydrothermal vent field where no H_2S occurred. Likewise, the O_2 microsensor signals recorded on the ocean floor outside hydrothermal activity were related to the corresponding O_2 concentration and the calibration data accordingly adjusted. The O_2 concentration of the nonhydrothermal bottom water was determined by Winkler titration on a ROV recovered water sample [*Hansen*, 1999]. All data sets were carefully inspected for outlying data by applying a filtering algorithm.

2.5. Long-Term Temperature Measurements

[18] For long-term measurements of temperatures above mussel beds, a miniaturized temperature data logger (MTL; described by *Pfender and Villinger* [2002]) was deployed immediately after the measurements with the ISI. The MTL was placed directly on top of the mussel bed for 130 h (5.5 days) at Site 2 (Figure 1) and monitored the temperature at 10 s intervals with 0.001°C resolution and an absolute accuracy of ±0.1°C.

[19] For long-term measurements of temperature inside mussel beds at high temporal and spatial resolutions, sensor lances were designed. Eight temperature sensors were installed at 4 cm intervals over a total length of 28 cm inside a steel tube and connected to an autonomous data logger. Each sensor was calibrated to a total precision of ±0.005°C. These lances were deployed in 2005 during the Hydromar II cruise (R/V *Meteor*, M64/2) using the ROV Quest [*Lackschewitz et al.*, 2005]. At Irina II, one such sensor lance was placed horizontally inside a mussel bed at the southeastern end of the mound in close proximity to the small active black smoker and a few meters away from the earlier ISI measurement at Site 2 (Figures 1 and 2c). The sensor lance was inserted approximately 10 cm underneath the top of the mussel bed and had an inclination of approximately 20° so that the tip of the lance was located about 20 cm below the top of the mussel bed. Temperatures were monitored at the 8 sensors simultaneously over a period of 250 days at one minute time intervals, resulting in a total of 2.8 million samples. All data were stored inside the data logger. After 20 months on the seafloor the loggers were recovered in 2007 during the Hydromar III cruise (R/V *Maria S. Merian*, MSM 04/3 [*Borowski et al.*, 2007]) using the ROV Jason II (Woods Hole Oceanographic Institute, Figure 2d).

2.6. Data Storage

[20] Data from this study were deposited in the Pangaea database (www.pangaea.de) and can be accessed under http://doi.pangaea.de/10.1594/PANGAEA.763153.

3. Results

3.1. Recordings of the in Situ Instrument

[21] During four ROV dives, each of which explored the Logatchev vent field for approximately 6 h, data from 6 sites were collected at time

intervals of one second (Tables 1 and 2). The bottom water temperature at approximately 3,000 m water depth outside of the area of hydrothermal influence was 2.6°C with a corresponding mean dissolved oxygen concentration of 232 μM. The highest temperature of 26.8°C was measured at the mussel-free Irina I site close to the rim of a smoking crater (Site 6). Correspondingly, the highest concentrations of dissolved H_2S and the lowest O_2 concentrations were measured at this site (Figures 3 and 4).

[22] Compared to ambient seawater, physicochemical conditions approximately 10 cm above mussel beds at Irina II (Site 1–5) were generally characterized by elevated temperatures, with slightly reduced oxygen and increased hydrogen sulfide concentrations (Figure 4 and Table 2). A temperature maximum of 7.4°C concurrent with a maximum of dissolved H_2S (156 μM) and a minimum of dissolved O_2 (142 μM) was recorded at Site 1A over mussel beds at a chimney base (Figure 5a). Similar conditions were found at Site 2 at the lower edge of an extended mussel bed with temperature and H_2S maxima of 6.0°C and 94 μM, respectively (Figure 5b). There was less variability in temperature and oxygen and hydrogen sulfide concentrations at the two other mussel beds investigated at Sites 3 and 4. Above a pillar-like structure densely overgrown with mussels (Site 3) and a small mussel patch (Site 4) temperatures did not exceed 3.9°C and 3.4°C, respectively, while the highest recorded concentrations of dissolved H_2S were 64 μM and 66 μM, respectively (Figures 5c and 5d). In comparison, at a chimney wall populated with alvinocarid shrimp but free of mussels (Site 5) the ISI recorded a temperature of 3.3°C and 48 μM dissolved H_2S (Figure 5e).

[23] Temperatures recorded with the ISI generally fluctuated noticeably within seconds at all investigated sites (Figures 3 and 5) with local minima close to ambient seawater. Mean temperatures never exceeded 3.0 ± 0.4°C (chimney base at Site 1) and 3.5 ± 0.7°C (mussel bed at Site 2) and were only 2.7 ± 0.1 to 2.8 ± 0.2°C at Sites 3–5. Mean dissolved H_2S concentrations ranged from 9 ± 7 μM to 31 ± 13 μM at these sites. The mean O_2 concentrations at all sites were between 216 ± 16 μM and 228 ± 9 μM (Figure 4 and Table 2).

3.2. Correlation of Temperature With H_2S and O_2 Based on ISI Microhabitat Measurements

[24] The H_2S microsensors used in this study did not respond ideally to changes in H_2S concentrations (i.e., in the order of seconds) and returned only slowly to the baseline after they were removed from the mussel habitats (i.e., in the order of 5 to 45 min depending on the physicochemical dynamics of the investigated site). Nevertheless, their response was fast enough to observe a clear time synchronicity between increases in temperature and dissolved H_2S concentrations and to detect positively correlated sulfide-temperature ratios (Figures 3 and 5). H_2S-T ratios were in the range of 2 to 60 μM H_2S/°C and increased threefold to fourfold when the regression line was forced through 2.6°C, the temperature of the sulfide-free ambient seawater. However, H_2S-T ratios had only weak determination coefficients ($R^2 \leq 0.31$, forced regressions $R^2 = 0.00$ in all but one cases) and were thus only very weakly supported (Figures 3 and 5 and Table 2). Therefore, no reliable sulfide-temperature ratios could be retrieved from the data. The response of the O_2 sensors was faster so that their profiles exactly mirrored temperature profiles, as visible in a strongly negative (−6 to −47 μM O_2/°C) and linear (determination coefficient R^2 = 0.40–0.83) correlation of O_2 with temperature (Figure 5). The result of the linear regressions between O_2 and temperature (i.e., the O_2-T ratio) was variable and depended on the range of temperature variation: the narrower the temperature range the more negative the ratio (Figure 6). For the sulfide pillar at Site 3 (2.6–3.9°C), the mussel patch at Site 4 (2.6–3.4°C), and the chimney wall at Site 5 (2.6–3.3°C), the O_2-T ratios were similar and in the range of −47 to −35 μM/°C. The O_2-T ratios for the chimney base at Site 1 (2.8–7.4°C), the mussel bed at Site 2 (2.7–6.0°C), and the rim of the smoking crater at Site 6 (2.6–26.8°C) were less negative and ranged from −24 to −6 μM O_2/°C (Table 2).

3.3. Long-Term Temperature Measurements

[25] Following the ISI deployment at Site 2, a miniaturized temperature logger (MTL) was placed on top of the mussel bed at the same site (Figure 5b) and recorded the temperature for 5.5 days. During the initial 4 days of the MTL deployment we recorded a mean temperature of 4.1°C ± 0.5°C (total range from 2.8°C to 6.3°C). This is consistent with the ISI temperature recordings at this site (Figure 4). After the fourth day the temperature suddenly dropped to a mean of 3.0°C ± 0.1°C with a maximum of 3.4°C and a minimum of 2.7°C and remained at this temperature until the end of recording (Figure 7). Based on the ISI data set from Site 2 and the resulting oxygen to temperature ratio of −6 μM O_2/°C, the oxygen concentration above the mussels at this site

Table 2. Mean, Minima, and Maxima of Distinct in Situ Measurements at Mussel Populations

		Temperature[a]				Dissolved O_2[b]						Dissolved H_2S							
Site	n	Med (°C)	Min (°C)	Max (°C)	Mean (°C)	Med (μM)	Min[c] (μM)	Max[c] (μM)	Mean (μM)	O_2-T ratio (μM/°C)	R^2	Sensor	Med (μM)	Min[c] (μM)	Max[c] (μM)	Mean (μM)	H_2S-T ratio (μM/°C)	R^2	Figure
1A, chimney colonized with mussels (base)	6,656	2.8	2.7	7.4	3.0 ± 0.4	230	206	242	228 ± 9	−16	0.584	S1	10	0	33	14 ± 10	2	0.006	Figure 5a
												S2	13	4	45	17 ± 11	−0.3	0.000	
1B, chimney colonized with mussels (top)	661	3.0	2.7	6.9	3.4 ± 0.9	222	178	232	216 ± 16	−14	0.813	S1	11	0	35	15 ± 12	−2	0.034	Figure 5a
												S2	7	2	28	9 ± 7	−3	0.094	
2, mussel bed	1,220	3.3	2.7	6.0	3.5 ± 0.7	218	200	228	218 ± 7	−6	0.400	S1	28	0	46	27 ± 12	8	0.109	Figure 5b
												S2	23	0	37	20 ± 8	6	0.111	
3, sulfide pillar overgrown with mussels	451	2.7	2.6	3.9	2.7 ± 0.2	229	203	233	227 ± 8	−39	0.813	S1	27	0	41	25 ± 10	18	0.023	Figure 5c
												S2	23	0	37	22 ± 11	24	0.045	
4A, mussel patch	345	2.7	2.6	3.4	2.8 ± 0.1	227	216	230	226 ± 5	−35	0.828	S1	31	4	50	31 ± 13	47	0.077	Figure 5d
												S2	failed						
4B, mussel patch	181	2.8	2.7	3.0	2.8 ± 0.1	225	215	231	225 ± 4	−47	0.823	S1	16	3	25	15 ± 7	60	0.313	Figure 5d
												S2	failed						
5, chimney wall populated with shrimp	224	2.8	2.6	3.3	2.8 ± 0.2	223	206	232	222 ± 7	−37	0.822	S1	30	8	54	29 ± 12	52	0.251	Figure 5e
												S2	failed						
6, rim of smoking crater	1,435	3.1	2.6	26.8	4.8 ± 3.7	200	32	235	181 ± 61	−27	0.670	S1	14	0	293	38 ± 110	33	0.243	Figure 3
												S2	17	0	136	28 ± 40	5	0.190	

[a]Ambient seawater temperature was 2.62°C.
[b]Ambient mean seawater oxygen concentration was 232 μM.
[c]Minimum and maximum values of dissolved O_2 and H_2S are defined as the 3% and 97% percentiles to account for the core data of the data set and to eliminate outlying data peaks. Med, median; mean is given ± standard deviation; S1 and S2, H_2S sensors 1 and 2.

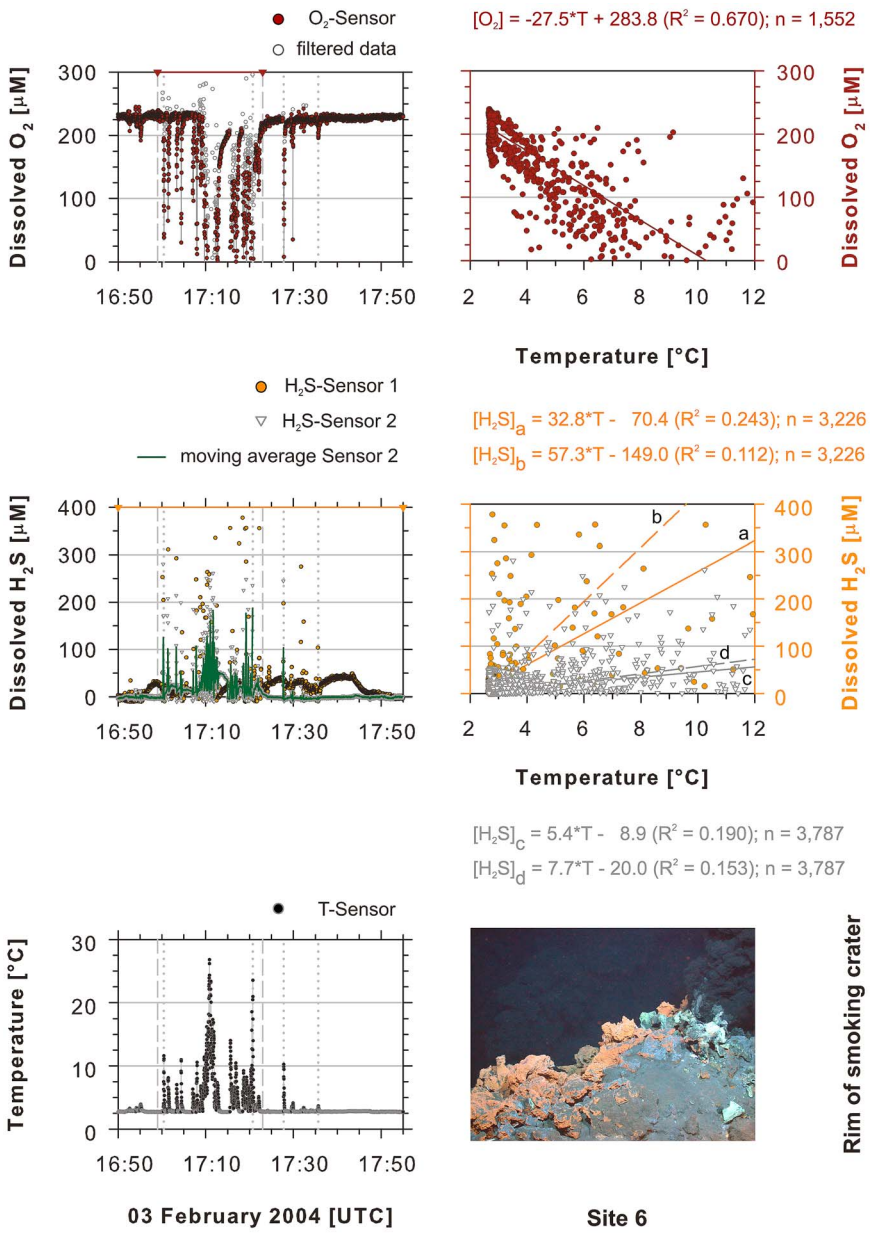

Figure 3. ISI recordings at Irina I at the rim of a smoking crater. Dashed lines indicate the time interval during which the ISI remained in the same location. Arrows at the top of the O_2 and H_2S plots mark the time interval examined for correlation with temperature. Note that temperature peaks are correlated with H_2S maxima and O_2 minima (dotted line). Time is given according to universal time code. The dashed lines (lines b and d) in the H_2S-T plot are the regression lines forced to 2.6°C (sulfide-free ambient seawater). Photograph copyright, MARUM University of Bremen.

was calculated from the MTL temperature recordings to have a mean of 225 ± 4 μM with a minimum of 210 μM at 6.3°C and a maximum of 232 μM at 2.7°C (Figure 7).

[26] After the ISI and MTL deployments, an 8-channel temperature lance was pushed horizontally into a mussel bed in close proximity to the preceding ISI and MTL measurements at Site 2 (Figures 1, 2c, and 8). The sensor lance was inserted approximately 10 cm into the mussel bed at an angle of approximately 20° so that the tip of the lance was located about 20 cm below the surface of the mussel bed. Over a length of 16 cm (corresponding to a vertical depth of ~10–16 cm) the temperature lance recorded temperature fluctuations between 2.7°C

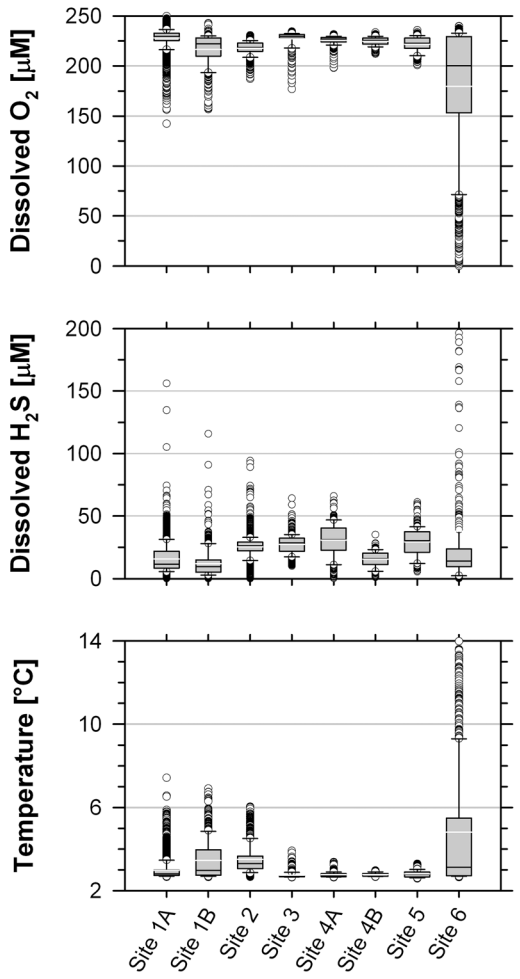

Figure 4. Box plot summary of ISI recordings. (top) Dissolved O_2, (middle) dissolved H_2S, and (bottom) temperature. The solid black line inside the gray boxes represents the median of the data. Grey boxes give the lower and upper quartiles of recorded data (i.e., 25th and 75th percentiles); whiskers show the 10th and 90th percentiles. Open circles represent the remaining data points below the 10th and above the 90th percentiles. The mean is shown as a solid white line inside the boxes.

and 15.8°C, however, 96% of all data (3% percentile to 97% percentile) were in the range of 3.0°C to 7.1°C. At the tip of the lance at 28 cm (i.e., 20 cm below the mussel bed surface) a temperature maximum of 18.2°C was recorded and the 3% to 97% percentiles were in the range of 3.3 to 16.0°C. Correspondingly, the mean temperatures increased from 3.8 ± 0.6°C to 4.4 ± 1.1°C 10–16 cm below the mussel bed surface, while higher mean temperatures of 8.3 ± 2.6°C and 10.9 ± 3.4°C were recorded 18 and 20 cm below the mussel bed surface (Figure 9 and Table 3). This indicates that the deeper mussel layers at the tip of the sensor lance were closer to the source of fluid flow and illustrates the small-scale spatial gradients that exist in mussel beds.

4. Discussion

4.1. Sulfide Above Mussel Beds

[27] The ISI recordings at the Irina II site of the Logatchev hydrothermal vent field revealed mean dissolved H_2S concentrations between 9 μM and 31 μM, mean dissolved O_2 concentrations between 216 μM and 228 μM, and mean temperatures between 2.8 and 3.5°C approximately 10 cm above the mussel beds (Figure 4 and Table 2). These data show that the mussels at Logatchev have simultaneous access to both dissolved H_2S and oxygen and indicate that their diffuse flow habitats provide sufficient concentrations of electron donors and acceptors for the mussel symbionts to gain energy through aerobic sulfide oxidation. The coexistence of H_2S and oxygen in diffuse flow areas is in agreement with previous observations [*Johnson et al.*, 1986b, 1988b; *Luther et al.*, 2008; *Mullaugh et al.*, 2008; *Nees et al.*, 2009, 2008; *Podowski et al.*, 2009, 2010] and does not contradict sulfide oxidation kinetics per se. The half-life for free sulfide oxidation ($H_2S + HS^-$) in air saturated seawater is about 26 h at 25°C and pH 8.0 [*Millero et al.*, 1987] and increases toward lower temperatures and lower oxygen concentrations to about 380 h at 2°C, pH 7.8, and 110 μM O_2 [*Johnson et al.*, 1994]. In fact, the reaction of H_2S with O_2 is thermodynamically unfavorable at all pH so both species can coexist [*Luther*, 2010]. Clearly, sulfide oxidation kinetics is significantly accelerated in the presence of metal ions which act as strong catalysts. For example, *Snavely and Blount* [1969] and *Chen and Morris* [1972] found that metal ions such as Ni^{2+}, Co^{2+}, Mn^{2+}, Cu^{2+}, Fe^{2+}, all of which are abundant in Logatchev end-member fluids [*Schmidt et al.*, 2007], increase the sulfide oxidation rate 45 to 100 fold. However, molecules must meet in order to react and catalysts must be present at exactly the same time and place to catalyze the reaction efficiently. At 2.5 mM H_2S in the end-member fluid and metal ions in micromolar concentrations (except for ferrous iron, see below) [*Schmidt et al.*, 2007], sulfide oxidation at Logatchev is apparently not fast enough to cause the complete removal of free sulfide. Thus, metal ion concentrations at Logatchev are not high enough to prohibit the coexistence of H_2S and O_2 in *Bathymodiolus* mussel beds. In brief, sulfide oxidation kinetics predicts that H_2S and O_2 can potentially coexist even in the presence of metal ions.

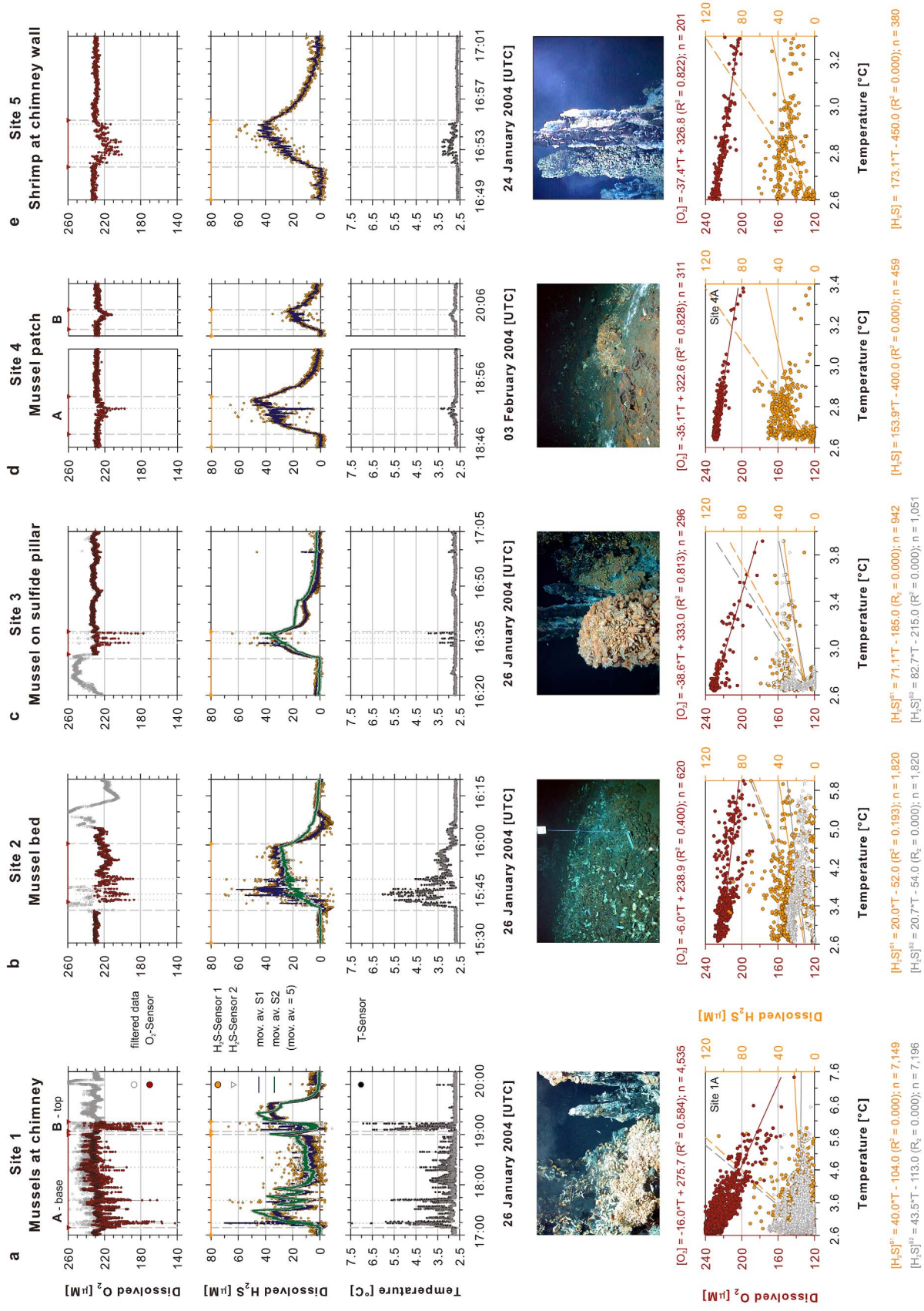
a
Site 1
Mussels at chimney
b
Site 2
Mussel bed
c
Site 3
Mussel on sulfide pillar
d
Site 4
Mussel patch
e
Site 5
Shrimp at chimney wall
A - base
B - top
filtered data
O2-Sensor
H2S-Sensor 1
H2S-Sensor 2
mov. av. S1
mov. av. S2
(mov. av. = 5)
T-Sensor
Dissolved O2 [µM]
Dissolved H2S [µM]
Temperature [°C]
26 January 2004 [UTC]
03 February 2004 [UTC]
24 January 2004 [UTC]
Site 1A
Site 4A
Temperature [°C]
[O2] = -16.0*T + 275.7 (R² = 0.584); n = 4,535
[O2] = -6.0*T + 238.9 (R² = 0.400); n = 620
[O2] = -38.6*T + 333.0 (R² = 0.813); n = 296
[O2] = -35.1*T + 322.6 (R² = 0.828); n = 311
[O2] = -37.4*T + 326.8 (R² = 0.822); n = 201
[H2S]f1 = 40.0*T - 104.0 (R² = 0.000); n = 7,149
[H2S]f2 = 43.5*T - 113.0 (R2 = 0.000); n = 7,196
[H2S]f1 = 20.0*T - 52.0 (R² = 0.193); n = 1,820
[H2S]f2 = 20.7*T - 54.0 (R2 = 0.000); n = 1,820
[H2S]f1 = 71.1*T - 185.0 (R2 = 0.000); n = 942
[H2S]f2 = 82.7*T - 215.0 (R² = 0.000); n = 1,051
[H2S]f1 = 153.9*T - 400.0 (R² = 0.000); n = 459
[H2S] = 173.1*T - 450.0 (R² = 0.000); n = 380

Figure 5

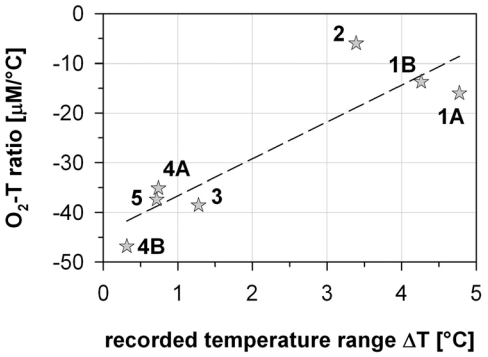

Figure 6. Correlation between the oxygen-temperature ratios and the recorded temperature range. The numbers next to the stars refer to the investigated sites.

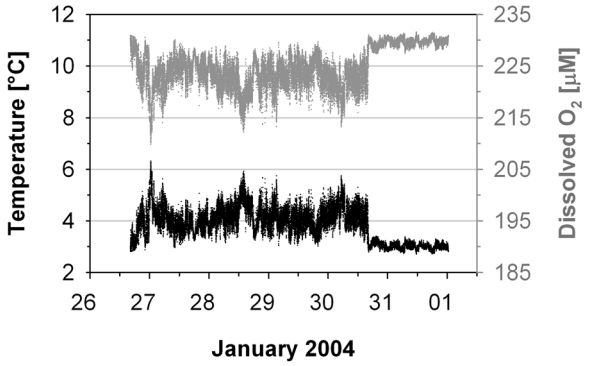

Figure 7. Long-term temperature and extrapolated oxygen conditions above the mussel bed at Site 2. Using a miniaturized temperature logger (MTL), the temperature was monitored for 128 h at sampling intervals of 10 s (n = 46,158). Based on the oxygen to temperature ratio resulting from the ISI measurements preceding the MTL deployment, the oxygen conditions (gray) were calculated from the MTL recordings (black). Time is given according to universal time code.

Notably, in Logatchev mussel beds H_2S and O_2 are not mutually exclusive.

[28] The wealth of dissolved H_2S in Logatchev diffuse flow habitats is in contrast to the extremely low free sulfide concentrations at Rainbow. At Rainbow, in situ measurements in diffuse fluids dominated by the shrimp *Rimicaris exoculata* had total sulfide concentrations (H_2S + HS^- + FeS) below 5 μM [*Schmidt et al.*, 2008]. This may not be surprising as fluids in the ultramafic-hosted Rainbow hydrothermal system are extremely rich in ferrous iron (Fe^{2+}) and precipitate most of the sulfide [*Le Bris and Duperron*, 2010]. Indeed, Rainbow high temperature fluids have an Fe-H_2S ratio of 24 [*Charlou et al.*, 2002; *Douville et al.*, 2002] and the Fe-H_2S ratio exceeds 30 in the shrimp environment [*Schmidt et al.*, 2008]. In the immediate surrounding of mussels, the iron concentration can exceed 100 μM and iron sulfide almost completely dominates sulfide speciation so that free sulfide is below detection levels at Rainbow [*Le Bris and Duperron*, 2010]. In contrast, ferrous iron concentrations at Logatchev are in the range of those reported from basalt-hosted vent systems on the MAR and the Fe-H_2S ratio is about 1 [*Le Bris and Duperron*, 2010; *Schmidt et al.*, 2007]. This indicates that sulfide (H_2S + HS^-) may not be fully precipitated by Fe^{2+}. Our data clearly show that dissolved H_2S is abundant in Logatchev diffuse fluids and imply that H_2S is neither fully precipitated nor otherwise completely removed by ferrous iron.

[29] In contrast to our in situ measurements, shipboard analyses of diffuse fluids after discrete sampling indicated fivefold to twelvefold lower sulfide concentrations in Irina II diffuse fluids. *Schmidt et al.* [2007] reported a maximum of 6.0 μM free sulfide (H_2S + HS^-) which corresponds to 2.7 μM

Figure 5. ISI recordings, O_2-T, and H_2S-T ratios at Sites 1–5. The ISI was moved horizontally toward the investigated sites. Dashed lines indicate the time interval during which the ISI remained in the same mussel habitat (time according to universal time code). Dotted lines emphasize the simultaneous sensing of prominent temperature and oxygen changes in diffuse fluids (peaks) together with slightly offset H_2S amplitudes. In the O_2 plots, dark red filled circles show the oxygen concentrations, while gray open circles indicate data that have been filtered and removed from the data set. Arrows at the top of the plot mark the time interval examined for correlation with temperature. In the H_2S plots, orange filled circles and gray triangles are the H_2S concentrations measured independently by two H_2S microsensors. The blue and dark green curves show the moving average over 5 s, i.e., 5 measurements. Arrows at the top of the plot mark the time interval examined for correlation with temperature. In the O_2-T and H_2S-T plots (below the photographs), the left axis (dark red) refers to O_2 concentrations (120–240 μM), while the right axis (orange) shows H_2S concentrations (0–120 μM). Symbols and colors are the same as in the O_2 and the H_2S plots. Solid lines in these plots are regular linear regressions, while dashed lines are H_2S-T regressions forced through 2.6°C (sulfide-free ambient seawater). Regression equations above the plots are for the O_2-T correlation, whereas equations below the plots show the forced H_2S-T regressions. For standard H_2S-T ratios see Table 2. Photographs copyright, MARUM University of Bremen.

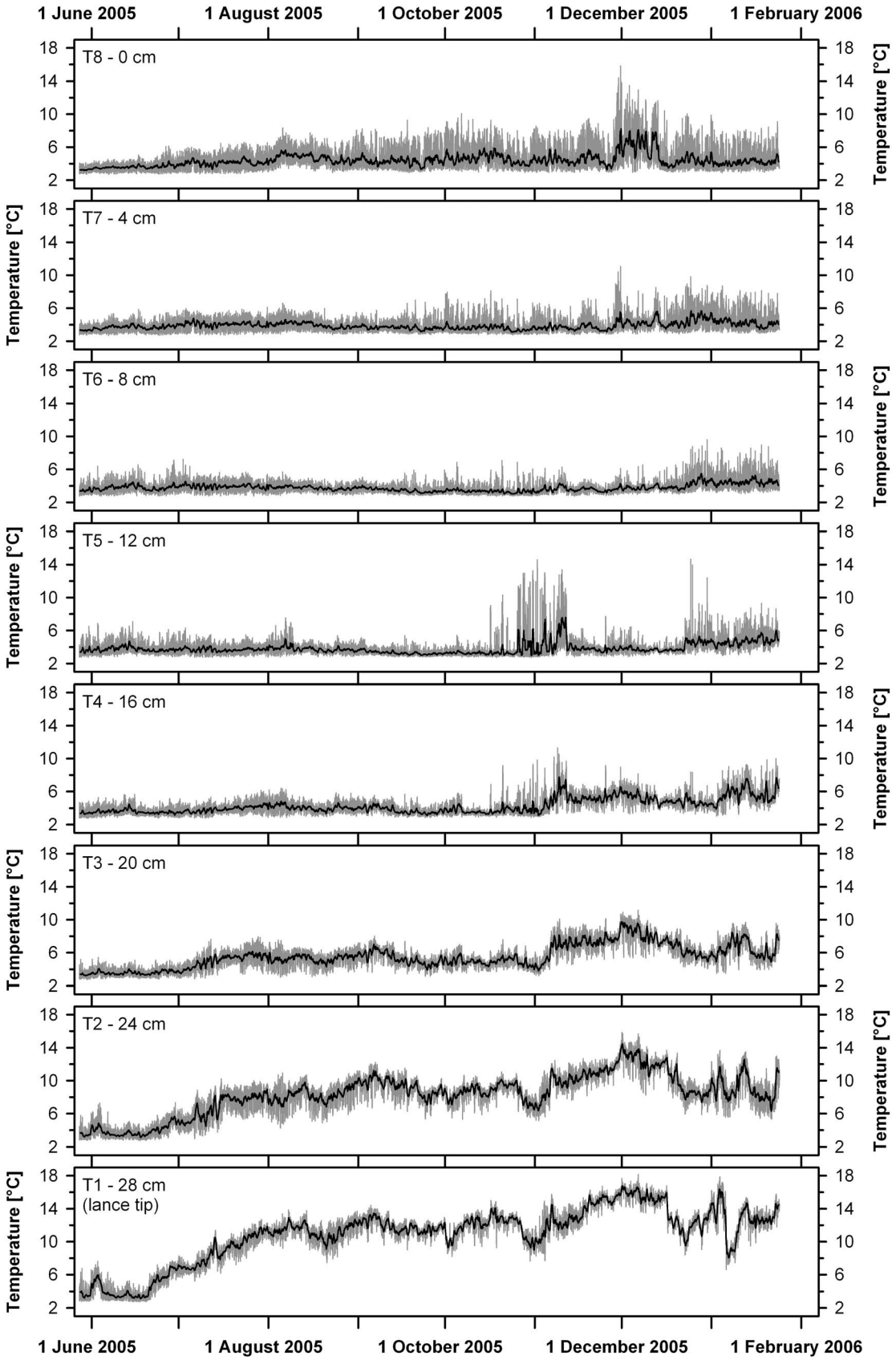
1 June 2005
1 August 2005
1 October 2005
1 December 2005
1 February 2006
T8 - 0 cm
T7 - 4 cm
T6 - 8 cm
T5 - 12 cm
T4 - 16 cm
T3 - 20 cm
T2 - 24 cm
T1 - 28 cm
(lance tip)
Temperature [°C]
18
14
10
6
2

Figure 8

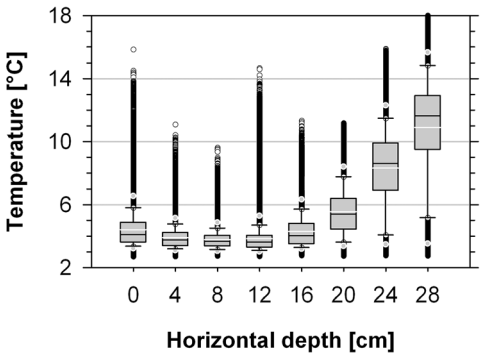

Figure 9. Box plot summary of the 8-channel temperature lance recordings. The solid black line inside the gray boxes represents the median of the data. Grey boxes show the lower and upper quartile of recorded data (i.e., 25th and 75th percentile); whiskers show the 10th and 90th percentiles and gray circles denote the 5th and 95th percentiles. The bold black line below the 10th and above the 90th percentile shows the range of the complete data set. Open white circles are discrete temperature maxima. The mean is shown as a solid white line inside the boxes.

dissolved H_2S at their reported pH (7.0) and an assumed in situ temperature of about 3.0°C [*Jeroschewski et al.*, 1996; *Millero et al.*, 1988]. This discrepancy between in situ and shipboard measurements after discrete sampling is most likely due to sulfide oxidation and/or precipitation during sample recovery, and has also been observed by others [*Le Bris et al.*, 2006a; *Schmidt et al.*, 2008].

[30] As the measured sulfide species in this study was dissolved H_2S our data are not directly comparable to free sulfide ($H_2S + HS^-$) or total sulfide ($H_2S + HS^- + FeS$) concentrations reported from basalt-hosted systems. However, concentrations of free sulfide can be calculated from dissolved H_2S concentrations if the pH, salinity, and temperature are also known [*Jeroschewski et al.*, 1996; *Millero et al.*, 1988]. In situ measurements of pH and salinity were attempted in this study using pH microsensors and a conductivity sensor but failed. Therefore, we can only estimate the free sulfide concentrations of Logatchev diffuse fluids: At mean temperatures of 2.8–3.5°C and an assumed pH range of 6.0 to 8.0 over *Bathymodiolus* mussel beds [*De Busserolles et al.*, 2009; *Sarradin et al.*, 1999b], mean dissolved H_2S concentrations of 9 to 31 μM correspond to mean free sulfide concentrations of 10–400 μM (pH 6.0: 10–35 μM, pH 6.5: 13–43 μM, pH 7.0: 20–69 μM, pH 7.5: 45–150 μM, pH 8.0: 122–408 μM). At basalt-hosted systems, free sulfide concentrations above mussel beds ranged from nondetectable to 87 μM, with mean concentrations of 27 μM [*Lutz et al.*, 2008; *Nees et al.*, 2008] (Table 4). Our estimates therefore indicate that free sulfide concentrations at the Logatchev vent field are in the same range as those reported from basalt-hosted vents.

4.2. Temperature Above and Inside Mussel Beds

[31] Maximum temperatures above and inside Logatchev mussel beds of 7.4°C (ISI, Site 1) and 18.2°C (T-lance) are consistent with maxima reported from other vent fields where maxima of around 20°C inside mussel beds have frequently been measured [*Chevaldonné et al.*, 1991; *Desbruyères et al.*, 2001; *Johnson et al.*, 1994; *Shank et al.*, 1998]. Temperature fluctuations with minima close to ambient as we report here are also in agreement with previous studies (Table 4).

[32] The mean temperatures at the Logatchev hydrothermal vent field (Irina II site) ranged from 2.8 ± 0.1°C to 3.5 ± 0.7°C above mussel beds and from 3.8 ± 0.6°C to 10.9 ± 3.4°C inside mussel beds, which is in agreement with temperature means reported from mussel beds at other hydrothermal vent fields. Mean temperatures between 5.7°C and 10.0°C have been reported for *B. azoricus* from Lucky Strike vent field on the slow spreading MAR [*Desbruyères et al.*, 2001; *Vuillemin et al.*, 2009]. *Johnson et al.* [1988a, 1994] reported mean temperatures between 3.0°C and 5.5°C above and inside clumps of *B. thermophilus* from the basalt-hosted Rose Garden vent field on the intermediate spreading Galapagos Rift whereas *Moore et al.* [2009] found the same species to prosper at average values between 1.6°C and 9.6°C at the fast spreading East Pacific Rise (9°50′N). Mean values between 5.5°C and 10.5°C have been reported from mussel beds in the Lau Back-Arc Basin [*Podowski et al.*, 2009, 2010] (Table 4).

[33] While the range of short-term fluctuations indicates a species' tolerance toward these variations, average values of environmental conditions reflect

Figure 8. Horizontal temperature distribution in a mussel bed monitored over 250 days. The temperature was measured about 10 cm below the surface of the mussel bed with 8 sensors (T1–T8) distributed over a distance of 28 cm. The gray plot shows the complete data set with a time resolution of 1 min (n = 2,784,440); the overlying black line is the 12 h mean of the temperature data.

Table 3. Mean, Minima, and Maxima of Long-Term Temperature Measurements 10–20 cm Inside a Mussel Bed Over a Horizontal Distance of 28 cm

	Channel							
	T8	T7	T6	T5	T4	T3	T2	T1
Horizontal depth (cm)	0.0	4.0	8.0	12.0	16.0	20.0	24.0	28.0
Vertical depth[a] (cm)	10.0	11.4	12.7	14.1	15.5	16.8	18.2	19.6
Minimum (°C)	2.7	2.7	2.7	2.7	2.8	2.7	2.8	2.7
1% percentile (°C)	3.0	3.0	2.9	2.9	3.0	3.1	3.1	3.1
3% percentile (°C)	3.1	3.0	3.0	3.0	3.1	3.3	3.3	3.3
5% percentile (°C)	3.2	3.1	3.0	3.0	3.2	3.4	3.5	3.5
10% percentile (°C)	3.3	3.2	3.1	3.1	3.3	3.6	4.1	5.2
25% percentile (°C)	3.6	3.4	3.4	3.3	3.5	4.4	6.9	9.5
Median (°C)	4.1	3.7	3.7	3.6	4.0	5.4	8.6	11.6
75% percentile (°C)	4.9	4.2	4.0	4.0	4.8	6.4	9.9	12.9
90% percentile (°C)	5.8	4.8	4.5	4.7	5.7	7.7	11.5	14.8
95% percentile (°C)	6.5	5.1	4.8	5.3	6.3	8.4	12.3	15.6
97% percentile (°C)	7.1	5.4	5.1	5.8	6.7	8.8	12.8	16.0
99% percentile (°C)	8.5	6.2	5.7	8.0	7.6	9.7	13.8	16.6
Maximum (°C)	15.8	11.1	9.6	14.7	11.3	11.2	15.9	18.2
Mean ± SD (°C)	4.4 ± 1.1	3.9 ± 0.7	3.8 ± 0.6	3.8 ± 0.9	4.3 ± 1.0	5.5 ± 1.5	8.3 ± 2.6	10.9 ± 3.4

[a]Vertical depth is approximate and relative to channel T8 at ~10 cm inside the mussel bed. (The sensor lance had an inclination of about 20°. Therefore, the tip of the sensor lance (channel T1) was deeper inside the mussel bed than the end of the lance (channel T8)). SD, standard deviation.

the general physicochemical situation to which a given species is exposed during part or most of its lifespan and are thus valuable environmental descriptors, particularly for hemisessile organisms such as bathymodiolin mussels. The long-term average temperatures at which bathymodiolin mussels have been regularly found rarely exceed 10°C (Table 4), although occasionally long-term average temperatures between 11°C and 17°C have been reported [*Chevaldonné et al.*, 1991; *Desbruyères et al.*, 2001; *Moore et al.*, 2009]. Interestingly, in respirometry experiments under nonoxygen limiting conditions, bathymodiolin mussels were able to survive sustained exposure to temperatures as high as 18°C [*Henry et al.*, 2008]. This indicates that the distribution of bathymodiolin mussels at hydrothermal vents is influenced more by their oxygen requirements than by their temperature tolerance. Correspondingly, mussels at Logatchev were generally exposed to temperatures below 10°C (Table 4), and extrapolation of temperature to an oxygen concentration of zero using the oxygen-temperature relationship observed at the rim of a smoking crater (Site 6) indicates that diffuse flow habitats at Logatchev become anoxic around this temperature (Figure 3).

4.3. Correlation of Temperature With H_2S and O_2 Based on Microhabitat Measurements

[34] *Johnson et al.* [1988a] showed that temperature can be used to estimate sulfide and oxygen concentrations in diffuse vent fluids. Temperatures of 2 to 11°C correlated positively with total sulfide (H_2S + HS^- + FeS) and negatively with oxygen although the relationship was not always linear due to biological consumption of these compounds [*Johnson et al.*, 1988a]. *Le Bris et al.* [2003, 2006a, 2006b] confirmed the linear relationship between sulfide and temperature, but pointed out that sulfide to temperature ratios are only constant at a given site and can be highly variable between sites. Temporal and spatial variability of sulfide-temperature ratios has recently been demonstrated using in situ voltammetry [*Nees et al.*, 2009, 2008]. Our data show that sulfide is positively correlated with temperature, however because of the slow response times and signal drifts of our H_2S microsensors, we were not able to reliably estimate sulfide-temperature ratios at Logatchev.

[35] Our study is the first in which in situ oxygen concentrations of fluids from an ultramafic-hosted hydrothermal vent were measured. O_2 profiles from all sites in the Logatchev vent field consistently mirrored temperature profiles and showed a strongly inverse linear correlation of O_2 with temperature. The ratio between oxygen and temperature varied between sites and ranged from −6 to −47 μM/°C. Temporal and spatial variability of oxygen-temperature ratios has also been shown in diffuse fluids of basalt-hosted hydrothermal vents using in situ voltammetry [*Moore et al.*, 2009; *Nees et al.*, 2008]. There are several explanations for this variability. First, bathymodiolin mussel beds laterally divert the flow of diffuse vent fluids, thereby diluting the fluid

Table 4. In Situ Sulfide, Oxygen, and Temperature Conditions of Various Hydrothermal Diffuse Flow Habitats in Comparison

Habitat	Field	Ridge	Year	Method	H_2S (μM)		$H_2S + HS^-$ (μM)		$H_2S + HS^- +$ FeS (μM)		O_2 (μM)		T (°C)		Reference
					Min–Max	Means	Min–Max	Means	Min–Max	Means	Min–Max	Means	Min–Max	Means	
Bathymodilus puteoserpentis	Logatchev	MAR	2004	EC/microsensors	0–54[a]	9–31	na	45–150[b]	na	na	178–242[a]	216–228	2.6–7.4[a]	2.8–3.5	This Study
Bathymodiolus azoricus	Lucky Strike	MAR	1998 and 2006	CM/FIA	na	na	na	na	0–67	1–9	ND	ND	4.4–14.2	5.7–10.0	1, 2
Bathymodiolus thermophilus	Rose Garden	GR	1985 and 1988	CM/CFA	na	na	na	na	0–330	-	0–110	-	2.1–14.0	3.0–5.5	3–7
	9°50′N	EPR	2002	CM/FIA	na	na	na	na	≤154	-	ND	ND	≤15	-	8
	9°50′N	EPR	2004–2007	EC/VM	na	na	0–87	0–109	na	na	3–187	48–105	2.0–7.9	1.6–9.6	9–11
Bathymodiolus brevior	Kilo Moana, Tow Cam, ABE, Tu'i Malila	ELSC	2005 and 2006	EC/VM	na	na	0–132	8–24	0–100	<30	0–200	100–150	2.4–32.0	5.5–10.5	12–15
Riftia pachyptila	13°N	EPR	1999	CM/FIA	na	na	na	na	3–31	-	ND	ND	2.0–8.0	-	16
	9°50′N	EPR	1999 and 2003–2008	EC/VM	na	na	0–498	13–80	5–100	-	≤3–150	37–52	2.0–69.0	6.9–12.0	17–19
Tevnia jerichonana	9°50′N	EPR	2006–2008	EC/VM	na	na	0–550	32–112	-	-	≤3–113	21–70	1.8–31.0	8.7–11.4	19
Rimicaris exoculata	Rainbow	MAR	2001 and 2005	CM/FIA	na	na	na	na	<5	-	ND	ND	5.3–18.2	6.2–16.0	20

[a]Minimum and maximum values of dissolved H_2S and O_2 are defined as the 3% and 97% percentiles to account for the core data of the data set and to eliminate outlying data peaks.
[b]Estimated range of means at pH 7.5. References: 1, *Desbruyères et al.* [2001]; 2, *Vuillemin et al.* [2009]; 3, *Johnson et al.* [1986b]; 4, *Fisher et al.* [1988]; 5, *Johnson et al.* [1988a]; 6, *Johnson et al.* [1988b]; 7, *Johnson et al.* [1994]; 8, *Le Bris et al.* [2006b]; 9, *Lutz et al.* [2008]; 10, *Nees et al.* [2008]; 11, *Moore et al.* [2009]; 12, *Mullaugh et al.* [2008]; 13, *Waite et al.* [2008]; 14, *Podowski et al.* [2009]; 15, *Podowski et al.* [2010]; 16, *Le Bris et al.* [2003]; 17, *Luther et al.* [2001a]; 18, *Luther et al.* [2008]; 19, *Nees et al.* [2009]; 20, *Schmidt et al.* [2008]. Abbreviations: na, not applicable; ND, not determined; dash, data not given; GR, Galapagos Rift; ELSC, East Lau Spreading Center; EPR, East Pacific Rise; MAR, Mid-Atlantic Ridge; CM, colorimetry; EC, electrochemistry; CFA, conventional flow analysis; FIA, flow injection analysis; VM, voltammetry.

and its components as it moves through the mussel beds by variable mixing with seawater [*Johnson et al.*, 1994, 1988b]. Second, mussels at Logatchev are likely supplied by multiple sources of diffuse venting from many small cracks in the ocean floor [*Petersen et al.*, 2009] which may also differ in their degree of dilution with ambient seawater. Third, deep ocean currents, tides, and local topography affect the flow of diffuse fluids and thus influence its relative composition over space and time [*Chevaldonné et al.*, 1991; *Johnson and Tunnicliffe*, 1985; *Little et al.*, 1988].

[36] Although a few studies have examined the relationship between temperatures of diffuse fluids and either their oxygen or their sulfide contents, little in situ data are available on the correlations between the three key variables temperature, oxygen, and sulfide at different vents and their effect on vent communities. *Johnson et al.* [1988a, 1994] showed that diffuse fluids at Rose Garden on the Galapagos Ridge became anoxic above 11°C. At this temperature sulfide concentrations (S_{tot}) were above 100 μM but never exceeded 200 μM. In contrast, diffuse fluids in the Lau Basin with average temperatures of 7–25°C were well oxygenized (60–150 μM) and contained comparably little sulfide (S_{free} = 8–70 μM) ([*Podowski et al.*, 2010] based on 332 survey locations containing chemosymbiotic macrofauna). In our study, *Bathymodiolus* mussels were generally found at mean temperatures below 6°C, so that these experienced oxygen concentration between 100 and 200 μM (depending on the site) and free sulfide concentrations of 10 to 400 μM (depending on the pH).

5. Conclusions

[37] At Logatchev, fluids became anoxic at around 10°C. The long-term average of temperatures inside Logatchev mussel beds were generally far below this value (Figures 8 and 9 and Table 3) indicating that over the monitored period of 250 days the mussels were neither oxygen limited nor overexposed to free sulfide. Noticeably, mussels were also not limited by sulfide availability as free sulfide was always present above the mussel beds, i.e., had not been completely chemically oxidized or biologically depleted during the ascent of the vent fluids through the mussel bed. Our data show that the Logatchev mussels have simultaneous access to both free sulfide and oxygen. Their diffuse flow habitats thus provide sufficient concentrations of electron donors and acceptors for the mussel symbionts to gain energy through aerobic sulfide oxidation.

[38] Our data confirm previous studies that physicochemical conditions in hydrothermal diffuse flow habitats can be highly variable at very small temporal and spatial scales. It is becoming increasingly apparent that each individual mussel lives in a temporally changing microenvironment that can differ in its physicochemical properties from the microenvironments of neighboring mussels. Direct in situ characterization of this microhabitat heterogeneity is highly challenging but worthwhile as it can reveal how spatial and temporal gradients in diffuse fluids affect the vent biota and thus contributes to our understanding of geosphere-biosphere interactions at hydrothermal vents.

Acknowledgments

[39] We gratefully acknowledge the chief scientists Thomas Kuhn, Klas Lackschewitz, and Christian Borowski of the involved research cruises as well as the crews of the research vessels *Meteor* and *Maria S. Merian* and the ROV's Quest and Jason II for their invaluable support. We thank Volker Meyer, Paul Färber, and Harald Osmers for their commitment during last minute adaptations of the in situ instrument for use with the ROV Quest. Ursula Werner and Eva Walpersdorf are acknowledged for their introduction to working with microsensors. We appreciate Gabriele Eickert who skillfully constructed the microelectrodes and gave indispensable comments for their deployment in the field. We are grateful to two anonymous reviewers who gave valuable comments for the improvement of this paper. This work was supported by the German Science Foundation (DFG) Priority Program 1144 "From Mantle to Ocean: Energy-, Material- and Life Cycles at Spreading Axes" (publication 61), the DFG Cluster of Excellence "The Ocean in the Earth System" at MARUM, Bremen, and the Max Planck Society.

References

Beaulieu, S. E. (2010), InterRidge global database of active submarine hydrothermal vent fields, version 2.1, Natl. Oceanogr. Cent., Southampton, U. K. [Available at http://www.interridge.org/IRvents.]

Bogdanov, Y. A., N. S. Bortnikov, I. V. Vikent'ev, E. G. Gurvich, and A. M. Sagalevich (1997), A new type of modern mineral-forming system: Black smokers of the hydrothermal field at 14°45′N latitude, Mid-Atlantic Ridge, *Geol. Ore Deposits*, *39*(1), 58–78.

Borowski, C., et al. (2007), Hydromar III: Temporal and spatial variability of hydrothermal, geochemical and biological systems at the Logatchev hydrothermal vent field, Mid-Atlantic Ridge at 14°45′N, *Maria S. Merian*, cruise no. 04, Leg 3, 1–159, Inst. für Meereskd. der Univ. Hamburg, Hamburg, Germany, doi:10013/epic.32341.d001.

Borowski, C., S. Petersen, and N. Augustin (2008), New coordinates for the hydrothermal structures in the Logatchev vent field at 14°45′N on the Mid-Atlantic Ridge: Supplement to

article in InterRidge News, Vol. 16, *InterRidge News*, *17*, 20. [Available at: http://www.interridge.org/IRNewsletter.]

Cannat, M., Y. Lagabrielle, H. Bougault, J. Casey, N. deCoutures, L. Dmitriev, and Y. Fouquet (1997), Ultramafic and gabbroic exposures at the Mid-Atlantic Ridge: Geological mapping in the 15°N region, *Tectonophysics*, *279*(1–4), 193–213, doi:10.1016/S0040-1951(97)00113-3.

Charlou, J. L., J. P. Donval, Y. Fouquet, P. Jean-Baptiste, and N. Holm (2002), Geochemistry of high H_2 and CH_4 vent fluids issuing from ultramafic rocks at the Rainbow hydrothermal field (36°14′N, MAR), *Chem. Geol.*, *191*(4), 345–359, doi:10.1016/S0009-2541(02)00134-1.

Chen, K. Y., and J. C. Morris (1972), Oxidation of sulfide by O_2: Catalysis and inhibition, *J. Sanit. Eng. Div., Am. Soc. Civ. Eng.*, *98*(1), 215–227.

Chevaldonné, P., D. Desbruyères, and M. Le Haître (1991), Time-series of temperature from three deep-sea hydrothermal vent sites, *Deep Sea Res., Part A*, *38*(11), 1417–1430, doi:10.1016/0198-0149(91)90014-7.

Cline, J. D. (1969), Spectrophotometric determination of hydrogen sulfide in natural waters, *Limnol. Oceanogr.*, *14*(3), 454–458, doi:10.4319/lo.1969.14.3.0454.

de Beer, D., E. Sauter, H. Niemann, N. Kaul, J. P. Foucher, U. Witte, M. Schlüter, and A. Boetius (2006), In situ fluxes and zonation of microbial activity in surface sediments of the Håkon Mosby Mud Volcano, *Limnol. Oceanogr.*, *51*(3), 1315–1331, doi:10.4319/lo.2006.51.3.1315.

De Busserolles, F., J. Sarrazin, O. Gauthier, Y. Gélinas, M. C. Fabri, P. M. Sarradin, and D. Desbruyères (2009), Are spatial variations in the diets of hydrothermal fauna linked to local environmental conditions?, *Deep Sea Res., Part II*, *56*(19–20), 1649–1664, doi:10.1016/j.dsr2.2009.05.011.

Desbruyères, D., et al. (2001), Variations in deep-sea hydrothermal vent communities on the Mid-Atlantic Ridge near the Azores plateau, *Deep Sea Res., Part I*, *48*(5), 1325–1346, doi:10.1016/S0967-0637(00)00083-2.

Di Meo-Savoie, C. A., G. W. Luther III, and S. C. Cary (2004), Physicochemical characterization of the microhabitat of the epibionts associated with *Alvinella pompejana*, a hydrothermal vent annelid, *Geochim. Cosmochim. Acta*, *68*(9), 2055–2066, doi:10.1016/j.gca.2003.10.039.

Douville, E., J. L. Charlou, E. H. Oelkers, P. Bienvenu, C. F. J. Colon, J. P. Donval, Y. Fouquet, D. Prieur, and P. Appriou (2002), The rainbow vent fluids (36°14′N, MAR): The influence of ultramafic rocks and phase separation on trace metal content in Mid-Atlantic Ridge hydrothermal fluids, *Chem. Geol.*, *184*(1–2), 37–48, doi:10.1016/S0009-2541(01)00351-5.

Duperron, S., C. Bergin, F. Zielinski, A. Blazejak, A. Pernthaler, Z. P. McKiness, E. DeChaine, C. M. Cavanaugh, and N. Dubilier (2006), A dual symbiosis shared by two mussel species, *Bathymodiolus azoricus* and *Bathymodiolus puteoserpentis* (Bivalvia: Mytilidae), from hydrothermal vents along the northern Mid-Atlantic Ridge, *Environ. Microbiol.*, *8*(8), 1441–1447, doi:10.1111/j.1462-2920.2006.01038.x.

Fisher, C. R., et al. (1988), Microhabitat variation in the hydrothermal vent mussel, *Bathymodiolus thermophilus*, at the Rose Garden vent on the Galapagos Rift, *Deep Sea Res., Part A*, *35*(10–11), 1769–1791, doi:10.1016/0198-0149(88)90049-0.

Gebruk, A. V., P. Chevaldonné, T. Shank, R. A. Lutz, and R. C. Vrijenhoek (2000), Deep-sea hydrothermal vent communities of the Logatchev area (14°45′N, Mid-Atlantic Ridge): Diverse biotopes and high biomass, *J. Mar. Biol. Assoc. U. K.*, *80*(3), 383–393, doi:10.1017/S0025315499002088.

Gebruk, A., M.-C. Fabri, P. Briand, and D. Desbruyères (2010), Community dynamics over a decadal scale at Logatchev, 14°45′N, Mid-Atlantic Ridge, *Cah. Biol. Mar.*, *51*(4), 383–388.

Geret, F., R. Riso, P. M. Sarradin, J. C. Caprais, and R. P. Cosson (2002), Metal bioaccumulation and storage forms in the shrimp, *Rimicaris exoculata*, from the Rainbow hydrothermal field (Mid-Atlantic Ridge); Preliminary approach to the fluid-organism relationship, *Cah. Biol. Mar.*, *43*(1), 43–52.

German, C. R., and K. L. Von Damm (2006), Hydrothermal processes, in *Treatise on Geochemisty*, vol. 6, *The Oceans and Marine Geochemistry*, edited by H. Elderfield, chap. 7, pp. 181–222, Elsevier, Amsterdam.

Hansen, H. P. (1999), Determination of oxygen, in *Methods of Seawater Analysis*, edited by K. Grasshoff, K. Kremling, and M. Ehrhardt, pp. 75–89, Wiley, Weinheim, Germany, doi:10.1002/9783527613984.ch4.

Henry, M. S., J. J. Childress, and D. Figueroa (2008), Metabolic rates and thermal tolerances of chemoautotrophic symbioses from Lau Basin hydrothermal vents and their implications for species distributions, *Deep Sea Res., Part I*, *55*(5), 679–695, doi:10.1016/j.dsr.2008.02.001.

Jeroschewski, P., C. Steuckart, and M. Kühl (1996), An amperometric microsensor for the determination of H_2S in aquatic environments, *Anal. Chem.*, *68*(24), 4351–4357, doi:10.1021/ac960091b.

Johnson, H. P., and V. Tunnicliffe (1985), Time-series measurements of hydrothermal activity on northern Juan de Fuca Ridge, *Geophys. Res. Lett.*, *12*(10), 685–688, doi:10.1029/GL012i010p00685.

Johnson, K. S., C. L. Beehler, and C. M. Sakamoto-Arnold (1986a), A submersible flow analysis system, *Anal. Chim. Acta*, *179*, 245–257, doi:10.1016/S0003-2670(00)84469-4.

Johnson, K. S., C. L. Beehler, C. M. Sakamoto-Arnold, and J. J. Childress (1986b), In situ measurements of chemical distributions in a deep-sea hydrothermal vent field, *Science*, *231*(4742), 1139–1141, doi:10.1126/science.231.4742.1139.

Johnson, K. S., J. J. Childress, and C. L. Beehler (1988a), Short-term temperature variability in the Rose Garden hydrothermal vent field: An unstable deep-sea environment, *Deep Sea Res. A*, *35*(10–11), 1711–1721, doi:10.1016/0198-0149(88)90045-3.

Johnson, K. S., J. J. Childress, R. R. Hessler, C. M. Sakamoto-Arnold, and C. L. Beehler (1988b), Chemical and biological interactions in the Rose Garden hydrothermal vent field, Galapagos spreading center, *Deep Sea Res. A*, *35*(10–11), 1723–1744, doi:10.1016/0198-0149(88)90046-5.

Johnson, K. S., J. J. Childress, C. L. Beehler, and C. M. Sakamoto (1994), Biogeochemistry of hydrothermal vent mussel communities: The deep-sea analogue to the intertidal zone, *Deep Sea Res., Part I*, *41*(7), 993–1011, doi:10.1016/0967-0637(94)90015-9.

Kühl, M., C. Steuckart, G. Eickert, and P. Jeroschewski (1998), A H_2S microsensor for profiling biofilms and sediments: Application in an acidic lake sediment, *Aquat. Microb. Ecol.*, *15*(2), 201–209, doi:10.3354/ame015201.

Kuhn, T., et al. (2004), The Logatchev hydrothermal field–revisited: Preliminary results of the R/V *Meteor* cruise Hydromar I (M60/3), *InterRidge News*, *13*, 1–4. [Available at: http://www.interridge.org/IRNewsletter.]

Lackschewitz, K. S., et al. (2005), Longterm study of hydrothermalism and biology at the Logatchev field, Mid-Atlantic Ridge at 14°45′N (revisit 2005; Hydromar II), Meteor Berichte 05, Mid-Atlantic Expedition 2005, cruise No. 64,

Leg 2, 1–171, Inst. für Meereskd. der Univ. Hamburg, Hamburg, Germany, doi:10013/epic.32337.d001.

Le Bris, N., and S. Duperron (2010), Chemosynthetic communities and biogeochemical energy pathways along the MAR: The case of *Bathymodiolus azoricus*, in *Diversity of Hydrothermal Systems on Slow Spreading Ocean Ridges*, *Geophys. Monogr. Ser.*, vol. 188, edited by P. Rona et al., pp. 409–429, AGU, Washington D. C.

Le Bris, N., P. M. Sarradin, D. Birot, and A. M. Alayse-Danet (2000), A new chemical analyzer for in situ measurement of nitrate and total sulfide over hydrothermal vent biological communities, *Mar. Chem.*, *72*(1), 1–15, doi:10.1016/S0304-4203(00)00057-8.

Le Bris, N., P. M. Sarradin, and J. C. Caprais (2003), Contrasted sulphide chemistries in the environment of 13°N EPR vent fauna, *Deep Sea Res., Part I*, *50*(6), 737–747, doi:10.1016/S0967-0637(03)00051-7.

Le Bris, N., M. Zbinden, and F. Gaill (2005), Processes controlling the physico-chemical micro-environments associated with Pompeii worms, *Deep Sea Res., Part I*, *52*(6), 1071–1083, doi:10.1016/j.dsr.2005.01.003.

Le Bris, N., P. Rodier, P. M. Sarradin, and C. Le Gall (2006a), Is temperature a good proxy for sulfide in hydrothermal vent habitats?, *Cah. Biol. Mar.*, *47*(4), 465–470.

Le Bris, N., B. Govenar, C. Le Gall, and C. R. Fisher (2006b), Variability of physico-chemical conditions in 9°50′N EPR diffuse flow vent habitats, *Mar. Chem.*, *98*(2–4), 167–182, doi:10.1016/j.marchem.2005.08.008.

Lilley, M. D., D. A. Butterfield, J. E. Lupton, and E. J. Olson (2003), Magmatic events can produce rapid changes in hydrothermal vent chemistry, *Nature*, *422*(6934), 878–881, doi:10.1038/nature01569.

Little, S. A., K. D. Stolzenbach, and F. J. Grassle (1988), Tidal current effects on temperature in diffuse hydrothermal flow: Guaymas basin, *Geophys. Res. Lett.*, *15*(13), 1491–1494, doi:10.1029/GL015i013p01491.

Luther, G. W., III (2010), The role of one- and two-electron transfer reactions in forming thermodynamically unstable intermediates as barriers in multi-electron redox reactions, *Aquat. Geochem.*, *16*(3), 395–420, doi:10.1007/s10498-009-9082-3.

Luther, G. W., III, T. F. Rozan, M. Taillefert, D. B. Nuzzio, C. Di Meo, T. M. Shank, R. A. Lutz, and S. C. Cary (2001a), Chemical speciation drives hydrothermal vent ecology, *Nature*, *410*(6830), 813–816, doi:10.1038/35071069.

Luther, G. W., III, B. T. Glazer, L. Hohmann, J. I. Popp, M. Taillefert, T. F. Rozan, P. J. Brendel, S. M. Theberge, and D. B. Nuzzio (2001b), Sulfur speciation monitored in situ with solid state gold amalgam voltammetric microelectrodes: Polysulfides as a special case in sediments, microbial mats and hydrothermal vent waters, *J. Environ. Monit.*, *3*(1), 61–66, doi:10.1039/b006499h.

Luther, G. W., III, et al. (2008), Use of voltammetric solid-state (micro)electrodes for studying biogeochemical processes: Laboratory measurements to real time measurements with an in situ electrochemical analyzer (ISEA), *Mar. Chem.*, *108*, 221–235, doi:10.1016/j.marchem.2007.03.002.

Lutz, R. A., et al. (2008), Interrelationships between vent fluid chemistry, temperature, seismic activity, and biological community structure at a mussel-dominated, deep-sea hydrothermal vent along the East Pacific Rise, *J. Shellfish Res.*, *27*(1), 177–190, doi:10.2983/0730-8000(2008)27[177:IBVFCT]2.0.CO;2.

Maas, P. A. Y., G. D. O'Mullan, R. A. Lutz, and R. C. Vrijenhoek (1999), Genetic and morphometric characterization of mussels (Bivalvia: Mytilidae) from mid-Atlantic hydrothermal vents, *Biol. Bull.*, *196*(3), 265–272, doi:10.2307/1542951.

Martinez, F., K. Okino, Y. Ohara, A.-L. Reysenbach, and S. K. Goffredi (2007), Back-arc basins, *Oceanography*, *20*(1), 116–127.

Massoth, G. J., and H. B. Milburn (1997), SUAVE (SUbmersible System Used to Assess Vented Emissions): A diverse tool to probe the submarine hydrothermal environment, paper presented at International Workshop on Marine Analytical Chemistry for Monitoring and Oceanographic Research, Inst. Univ. Eur. De la Mer, Brest, France, 17–19 Nov.

Millero, F. J., S. Hubinger, M. Fernandez, and S. Garnett (1987), Oxidation of H_2S in seawater as a function of temperature, pH, and ionic strength, *Environ. Sci. Technol.*, *21*(5), 439–443, doi:10.1021/es00159a003.

Millero, F. J., T. Plese, and M. Fernandez (1988), The dissociation of hydrogen sulfide in seawater, *Limnol. Oceanogr.*, *33*(2), 269–274, doi:10.4319/lo.1988.33.2.0269.

Moore, T. S., T. M. Shank, D. B. Nuzzio, and G. W. Luther III (2009), Time-series chemical and temperature habitat characterization of diffuse flow hydrothermal sites at 9°50′N East Pacific Rise, *Deep Sea Res., Part II*, *56*(19–20), 1616–1621, doi:10.1016/j.dsr2.2009.05.008.

Mullaugh, K. M., G. W. Luther III, S. Ma, T. S. Moore, M. Yücel, E. L. Becker, E. L. Podowski, C. R. Fisher, R. E. Trouwborst, and B. K. Pierson (2008), Voltammetric (micro)electrodes for the in situ study of Fe^{2+} oxidation kinetics in hot springs and $S_2O_3^{2-}$ production at hydrothermal vents, *Electroanalysis*, *20*(3), 280–290, doi:10.1002/elan.200704056.

Nees, H. A., et al. (2008), Hydrothermal vent mussel habitat chemistry, pre- and post-eruption at 9°50′ North on the East Pacific Rise, *J. Shellfish Res.*, *27*(1), 169–175, doi:10.2983/0730-8000(2008)27[169:HVMHCP]2.0.CO;2.

Nees, H. A., R. A. Lutz, T. M. Shank, and G. W. Luther III (2009), Pre- and post-eruption diffuse flow variability among tubeworm habitats at 9°50′ north on the East Pacific Rise, *Deep Sea Res., Part II*, *56*(19–20), 1607–1615, doi:10.1016/j.dsr2.2009.05.007.

Petersen, S., K. Kuhn, T. Kuhn, N. Augustin, R. Hékinian, L. Franz, and C. Borowski (2009), The geological setting of the ultramafic-hosted Logatchev hydrothermal field (14°45′N, Mid-Atlantic Ridge) and its influence on massive sulfide formation, *Lithos*, *112*(1–2), 40–56, doi:10.1016/j.lithos.2009.02.008.

Pfender, M., and H. Villinger (2002), Miniaturized data loggers for deep sea sediment temperature gradient measurements, *Mar. Geol.*, *186*(3–4), 557–570, doi:10.1016/S0025-3227(02)00213-X.

Podowski, E. L., T. S. Moore, K. A. Zelnio, G. W. Luther III, and C. R. Fisher (2009), Distribution of diffuse flow megafauna in two sites on the Eastern Lau Spreading Center, Tonga, *Deep Sea Res., Part I*, *56*(11), 2041–2056, doi:10.1016/j.dsr.2009.07.002.

Podowski, E. L., S. Ma, G. W. Luther III, D. Wardrop, and C. R. Fisher (2010), Biotic and abiotic factors affecting distributions of megafauna in diffuse flow on andesite and basalt along the Eastern Lau Spreading Center, Tonga, *Mar. Ecol. Prog. Ser.*, *418*, 25–45, doi:10.3354/meps08797.

Revsbech, N. P. (1989), An oxygen microsensor with a guard cathode, *Limnol. Oceanogr.*, *34*(2), 474–478, doi:10.4319/lo.1989.34.2.0474.

Rozan, T. F., S. M. Theberge, and G. Luther III (2000), Quantifying elemental sulfur (S^0), bisulfide (HS^-) and polysulfides (S_x^{2-}) using a voltammetric method, *Anal. Chim. Acta*, *415*(1–2), 175–184, doi:10.1016/S0003-2670(00)00844-8.

Sakamoto-Arnold, C. M., K. S. Johnson, and C. L. Beehler (1986), Determination of hydrogen sulfide in seawater using flow injection analysis and flow analysis, *Limnol. Oceanogr.*, *31*(4), 894–900, doi:10.4319/lo.1986.31.4.0894.

Sarradin, P. M., N. Le Bris, D. Birot, and J. C. Caprais (1999a), Laboratory adaptation of the methylene blue method to flow injection analysis: Towards in situ sulfide analysis in hydrothermal seawater, *Anal. Commun.*, *36*(4), 157–160, doi:10.1039/a809759c.

Sarradin, P. M., J. C. Caprais, R. Riso, R. Kerouel, and A. Aminot (1999b), Chemical environment of the hydrothermal mussel communities in the Lucky Strike and Menez Gwen vent fields, Mid Atlantic ridge, *Cah. Biol. Mar.*, *40*(1), 93–104.

Schmidt, C., R. Vuillemin, C. Le Gall, F. Gaill, and N. Le Bris (2008), Geochemical energy sources for microbial primary production in the environment of hydrothermal vent shrimps, *Mar. Chem.*, *108*(1–2), 18–31, doi:10.1016/j.marchem.2007.09.009.

Schmidt, K., A. Koschinsky, D. Garbe-Schönberg, L. M. de Carvalho, and R. Seifert (2007), Geochemistry of hydrothermal fluids from the ultramafic-hosted Logatchev hydrothermal field, 15°N on the Mid-Atlantic Ridge: Temporal and spatial investigation, *Chem. Geol.*, *242*(1–2), 1–21, doi:10.1016/j.chemgeo.2007.01.023.

Shank, T. M., D. J. Fornari, K. L. Von Damm, M. D. Lilley, R. M. Haymon, and R. A. Lutz (1998), Temporal and spatial patterns of biological community development at nascent deep-sea hydrothermal vents (9°50′N, East Pacific Rise), *Deep Sea Res., Part II*, *45*(1–3), 465–515, doi:10.1016/S0967-0645(97)00089-1.

Snavely, E. S., and F. E. Blount (1969), Rates of reaction of dissolved oxygen with scavengers in sweet and sour brines, *Corrosion*, *25*(10), 397–404.

Snow, J. E., and H. N. Edmonds (2007), Ultraslow-spreading ridges: Rapid paradigm changes, *Oceanography*, *20*(1), 90–101.

Tivey, M. K. (2007), Generation of seafloor hydrothermal vent fluids and associated mineral deposits, *Oceanography*, *20*(1), 50–65.

Tunnicliffe, V., A. G. McArthur, and D. McHugh (1998), A biogeographical perspective of the deep-sea hydrothermal vent fauna, in *Advances in Marine Biology*, vol. 34, edited by J. H. S. Blaxter, B. Douglas, and P. A. Tyler, pp. 353–442, Academic, San Diego, Calif.

Van Dover, C. L. (2000), *The Ecology of Deep-Sea Hydrothermal Vents*, 424 pp., Princeton Univ. Press, Princeton, N. J.

Van Dover, C. L., and M. B. Doerries (2005), Community structure in mussel beds at Logatchev hydrothermal vents and a comparison of macrofaunal species richness on slow- and fast-spreading mid-ocean ridges, *Mar. Ecol.*, *26*(2), 110–120, doi:10.1111/j.1439-0485.2005.00047.x.

von Cosel, R., T. Comtet, and E. M. Krylova (1999), *Bathymodiolus* (Bivalvia: Mytilidae) from hydrothermal vents on the Azores Triple Junction and the Logatchev hydrothermal field, Mid-Atlantic Ridge, *Veliger*, *42*(3), 218–248.

Vuillemin, R., D. Le Roux, P. Dorval, K. Bucas, J. P. Sudreau, M. Hamon, C. Le Gall, and P. M. Sarradin (2009), CHEMINI: A new in situ CHEmical MINIaturized analyzer, *Deep Sea Res., Part I*, *56*(8), 1391–1399, doi:10.1016/j.dsr.2009.02.002.

Waite, T. J., T. S. Moore, J. J. Childress, H. Hsu-Kim, K. M. Mullaugh, D. B. Nuzzio, A. N. Paschal, J. Tsang, C. R. Fishers, and G. W. Luther III (2008), Variation in sulfur speciation with shellfish presence at a Lau Basin diffuse flow vent site, *J. Shellfish Res.*, *27*(1), 163–168, doi:10.2983/0730-8000(2008)27[163:VISSWS]2.0.CO;2.

Weiss, R. F. (1970), Solubility of nitrogen, oxygen and argon in water and seawater, *Deep Sea Res. Oceanogr. Abstr.*, *17*(4), 721–735, doi:10.1016/0011-7471(70)90037-9.

Wenzhöfer, F., and R. N. Glud (2002), Benthic carbon mineralization in the Atlantic: A synthesis based on in situ data from the last decade, *Deep Sea Res., Part I*, *49*(7), 1255–1279, doi:10.1016/S0967-0637(02)00025-0.

Wenzhöfer, F., O. Holby, R. N. Glud, H. K. Nielsen, and J. K. Gundersen (2000), In situ microsensor studies of a shallow water hydrothermal vent at Milos, Greece, *Mar. Chem.*, *69*(1–2), 43–54, doi:10.1016/S0304-4203(99)00091-2.

Wetzel, L. R., and E. L. Shock (2000), Distinguishing ultramafic- from basalt-hosted submarine hydrothermal systems by comparing calculated vent fluid compositions, *J. Geophys. Res.*, *105*(B4), 8319–8340, doi:10.1029/1999JB900382.